Supporting Information

First Supramolecular Sensors for Phosphonate Anions

Nina A. Esipenko,[a] Petr Koutnik,[a] Tsuyoshi Minami,[a] Lorenzo Mosca,[a] Vincent M. Lynch,[b] Grigory V. Zyryanov[a] and Pavel Anzenbacher Jr.*[a]

[a] *Department of Chemistry, Bowling Green State University, Bowling Green, Ohio 43403, USA. Fax: 419-372-9098; Tel: 419-372-2080; E-mail: pavel@bgsu.edu*
[b] *Department of Chemistry and Biochemistry, The University of Texas at Austin, Austin, TX, USA.*

Contents:

General

All syntheses were carried out under dry argon atmosphere using standard laboratory techniques. ^{1}H- and ^{13}C-NMR spectra were recorded on Bruker Avance III spectrometer at 500 MHz or 125 MHz, respectively at 25 °C with or without tetramethylsilane (TMS) as an internal reference. The chemical shifts (δ, ppm) are referenced to the respective solvent or TMS and splitting patterns are designated as s (singlet), d (doublet), t (triplet), q (quartet), m (multiplet), and bs (broad singlet). MALDI-TOF MS spectra were recorded using a Bruker Daltonics Omniflex spectrometer using dithranol or α-cyano-4-hydroxycinnamic acid as matrices. Electrospray Ionization (ESI) experiments were carried out using a Shimadzu 2010A LCMS instrument. Emission spectra were acquired at an Edinburgh single-photon counting spectrofluorometer FLSP 920 (Edinburgh Instruments Ltd, Livingston, U.K.). The spectra were obtained at room temperature using a quartz cuvette with a path length of 1 cm at right angle detection. The absorbance of all samples used for fluorescence studies were equal to or below 0.1. Absolute quantum yields were measured with a Hamamatsu absolute quantum yield spectrometer (Quantaurus-QY C11347, 150 W xenon lamp and multichannel detector/CCD sensor).

Column chromatography was performed on commercially available bulk flash silica gel 32-63u (Dynamic Adsorbents Inc., Norcross, GA, U.S.A.). Preparative thin-layer chromatography (TLC) was carried out on the Uniplate preparative silica gel TLC plates 2 mm, 20 × 20 cm with UV254 fluorescent dye (Analtech Inc., Newark, DE, U.S.A). 2-(trichloroacetyl)pyrrole was purchased from Aldrich, 4-(dimethylamino)-1 naphthyl-isothiocyanate from TCI America, 4-(phenanthro[9,10*d*]oxazol-2-yl)phenyl-isothiocyanate from Fluka, and the 4-tolylisothiocyanate was purchased from Acros Organics. All other reactants and reagents used in the syntheses were purchased from Aldrich, Fluka, or TCI America. The solvents methanol [(MeOH), *N,N*-dimethylformamide (DMF), diethylether (Et_2O), chloroform ($CHCl_3$), dichloromethane (DCM), and ethylacetate (EtOAc)] were purchased from EMD and used as received unless stated otherwise. All chemicals were used as received redundant. Tetrahydrofuran (THF) was distilled over Na/K alloy. Anhydrous dimethylsulfoxide (DMSO) was obtained using 4Å molecular sieves.

The array experiment was performed in 1536-well plates. The DMSO solutions of sensors were dispensed manually using Gilson micropipettes. Aqueous solutions of analytes were contact-free dispensed using BioRAPTR microfluidic robotic dispenser at 200 nL/s as follows. Each

experiment was performed in 24 repetitions. Each well received 6.3 µl of the sensor solution (10 µM) in DMSO, followed by 0.7 µl of the analyte solution (3 mM) in water. This way, final amount of water in DMSO is 10% (v/v). For control experiment, 0.7 µl of water was added instead of analyte solution. After the analyte solution was dispensed, the plate was centrifuged (2 min, 2500 rpm, 21 °C) and immediately read by a BMG PheraStar microplate reader using excitation at 450 nm, emission at 520 nm for **4** and **8**, excitation at 450 nm, emission at 550 nm for **6**, and excitation at 300 nm, emission at 450 nm for **5** and **7**. The resulting emission data were subjected to the student T-test to exclude 4 data-poins (of 24 repetitions). The coefficient of variability among the data within the class of 20 repetitions was lower than 3%. Thus obtained data for qualitative analysis were then analyzed using LDA without any further pretreatment.

Synthesis

Structures **1**, **2**, **3**, **6** and **8** were prepared according to published procedure. All analytical data were in an agreement with the published data. [1,2]

N,*N*'-(5-(aminomethyl)-2,4,6-triethyl-1,3-phenylene)bis(methylene)bis(1*H*-pyrrole-2-carboxamide) (9)

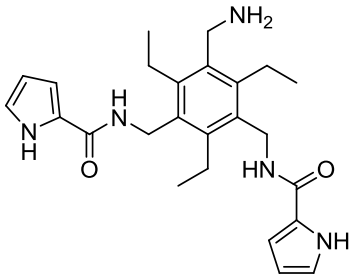

1,3,5-Tris(aminomethyl)-2,4,6-triethylbenzene (211 mg, 0.80 mmol) and 2-(trichloroacetyl)pyrrole (344 mg, 1.6 mmol) were dissolved in freshly distilled tetrahydrofurane (THF) in a vial. The vial was flushed with argon and screw-capped and the mixture was stirred at room temperature for 16 hours. The THF was then evaporated /co-distilled with toluene using a rotary evaporator and the white residue was dried *in vacuo*. Column chromatography (silica, 70 g, DCM/MeOH, 9 : 1 v/v, R_f = 0.14, isocratic elution) afforded product **9** (231 mg, 63 %). ^{1}H NMR (500 MHz, DMSO-d_6): δ = 11.45 (s, 2 H, HetN*H*), 7.84 (t, *J* = 4.5 Hz, 2 H, CON*H*), 6.83-6.82 (m, 4 H, Het*H*), 6.04-6.03 (m, 2 H, Het*H*), 4.48 (d, *J* = 4.5 Hz, 4 H, ArCH_2NH), 3.80 (s, 2 H, CH_2NH$_2$), 2.82-2.77 (m, 6 H, CH_2CH$_3$), 1.15-1.10 (m, 9 H, CH$_2$CH_3). ^{13}C-{^{1}H} NMR (125 MHz, DMSO-d_6): δ = 160.3, 143.0, 142.6, 135.6, 132.1, 126.1, 121.2, 110.7, 108.5, 38.6, 37.1, 22.7, 22.3, 16.5, 16.3. MS (MALDI-TOF): *m/z*= 458.28, [*M*+Na]$^+$ calcd. for $C_{25}H_{33}N_5NaO_2$ 458.25.

1,1',1''-(2,4,6-Triethylbenzene-1,3,5-triyl)tris(methylene)tris(3-(2-benzyl-1,3-dioxo-2,3-dihydro-1*H*-benzo[*de*]isoquinolin-6-yl)thiourea) (4)

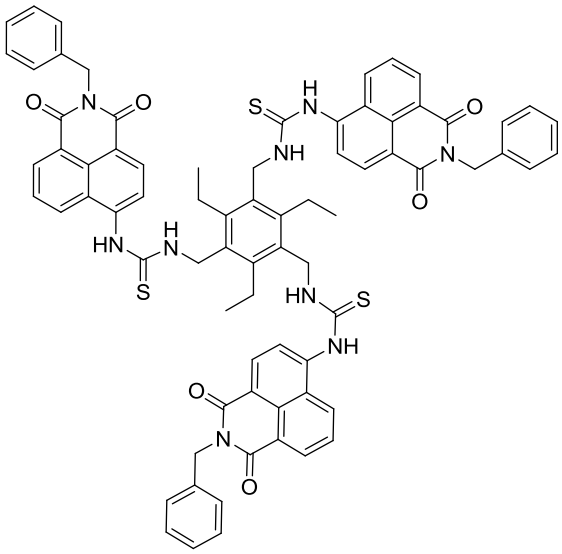

2-Benzyl-6-isothiocyanato-1*H*-benzo[*de*]isoquinoline-1,3(2*H*)-dione (300 mg, 0.87 mmol) was added to a tetrahydrofuran solution (100 mL) of 1,3,5-tris(aminomethyl)-2,4,6-triethylbenzene (48.3 mg, 0.19 mmol). The reaction mixture was stirred for 2 days at room temperature. The solvent was evaporated, and the residue was chromatographed on a silica using gradient of ethanol (0-10%, v/v) in chloroform as an eluent. 124 mg (50 %) of the **4** were obtained. M.p. > 175 ^{o}C (dec.). ^{1}H NMR (DMSO-d_6, 500 MHz): δ = 1.27 (t, J = 7.3 Hz, 9 H, CH_2CH_3), 2.88-2.89 (m, 6 H, CH_2CH_3), 4.87 (s, 6 H, $ArCH_2NH$), 5.25 (s, 6 H, $ArCH_2$), 7.22 (t, J = 7.3 Hz, 3 H, Ar*H*), 7.28 (t, J = 7.5 Hz, 6 H, Ar*H*), 7.33-7.35 (m, 6 H, Ar*H*), 7.89 (t, J = 8.0 Hz, 3 H, Ar*H*), 8.39 (bs, 3 H, CSN*H*), 8.47-8.54 (m, 12 H, Ar*H*), 10.08 (bs, 3 H, CSN*H*). ^{13}C-{^{1}H} NMR (125 MHz, DMSO-d_6): δ = 16.5, 23.12, 42.7, 42.9, 117.6, 122.2, 122.3, 125.9, 126.8, 127.1, 127.5, 128.4, 128.5, 128.9, 131.2, 131.4, 131.9, 137.4, 142.0, 144.4, 163.0, 163.6, 180.8. MS (MALDI-TOF): *m/z*= 1304.35, $[M+Na]^+$ calcd. for $C_{75}H_{63}N_9NaO_6S_3$ 1304.40.

1,1',1''-(2,4,6-triethylbenzene-1,3,5-triyl)tris(methylene)tris(3-(4-(dimethylamino) naphthalene-1-yl)thiourea) (5)

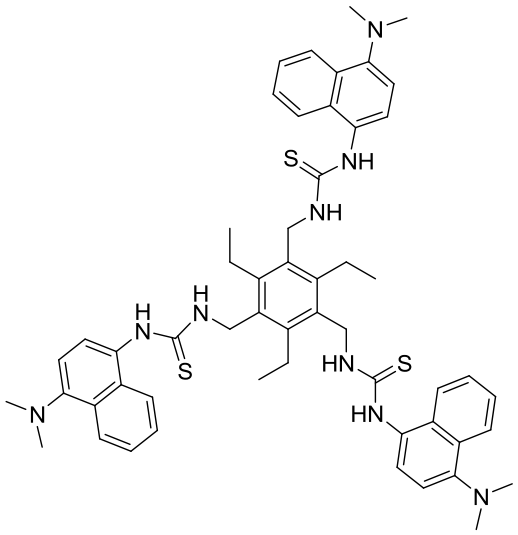

To a solution of 1,3,5-tris(aminomethyl)-2,4,6-triethylbenzene (53.8 mg, 0.22 mmol) in 7 ml of anhydrous THF in a vial (20 mL) under magnetic stirring, a solution of 4-(*N*,*N*-dimethylamino)napthalenisothiocyanate (257 mg, 1.1 mmol) in THF was added dropwise over 10 minutes. The vial was flushed with argon, screw-capped and covered with aluminum foil as the mixture was stirred at room temperature for 36 hours. The THF was then evaporated and the residue chromatographed on silica (25 g, toluene-acetone, 9 : 1 v/v, isocratic elution, R_f = 0.41 in toluene-acetone, 8 : 2 v/v). The product was isolated as a pale yellow solid (115 mg, 57 %). M.p. > 181 ^{o}C (dec.). ^{1}H NMR (DMSO-d_6, 500 MHz): δ = 9.32 (bs, 3 H, CSN*H*Ar), 8.18-8.16 (m, 3 H, Ar*H*), 7.86-7.84 (m, 3 H, Ar*H*), 7.56-7.51 (m, 6 H, Ar*H*), 7.47 (d, *J* = 7.8 Hz, 3 H, Ar*H*), 7.43 (bs, 3 H, CSN*H*CH$_2$), 7.10 (d, *J* = 8.1 Hz, 3 H, Ar*H*), 4.76 (bs, 6 H, ArC*H*$_2$NH), 2.81 (comp, 24 H, NC*H*$_3$ + C*H*$_2$CH$_3$), 1.15 (t, *J* = 7.1 Hz, 9 H, CH$_2$C*H*$_3$). ^{13}C-{^{1}H} NMR (125 MHz, DMSO-d_6): δ = 182.3, 149.2, 144.1, 132.2, 131.0, 129.6, 126.0, 125.5, 125.3, 124.2, 123.1, 113.6, 44.9, 42.8, 22.8, 16.5. MS (MALDI-TOF): *m/z*= 933.74, [*M*]$^{+}$ calcd. for $C_{54}H_{63}N_9S_3$ 933.44.

_N,N_'-(5-((3-(4-(Dimethylamino)naphthalen-1-yl)thioureido)methyl)-2,4,6-triethyl-1,3-phenylene)bis(methylene)bis(1_H_-pyrrole-2-carboxamide) (7)

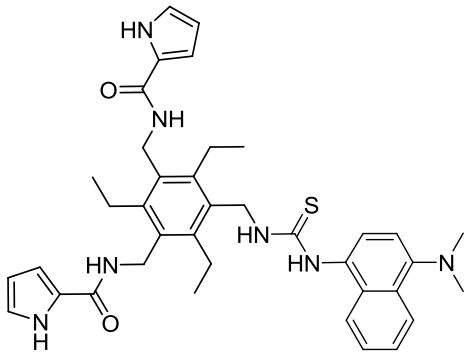

4-(*N*,*N*-Dimethylamino)napthalenisothiocyanate (32.1 mg, 0.14 mmol) was added in one portion to the solution of **9** (31.6 mg, 0.069 mmol) in 10 mL of freshly distilled THF upon stirring. The vial was flushed with argon, screw-capped and the mixture was stirred at room temperature for 15 hours. The white precipitate was filtered off using a paper filter, rinsed with THF and dried *in vacuo*. Compound **7** was isolated as a white powder (14 mg, 30 %). M.p. > 245 ^{o}C. ^{1}H NMR (500 MHz, DMSO-d_6): δ = 11.46 (bs, 2 H, HetN*H*), 9.37 (bs, 1 H, CSN*H*), 8.15-8.13 (m, 1 H, Ar*H*), 7.87 (t, *J* = 4.6 Hz, 2 H, Het*H*), 7.82 (d, *J* = 7.3 Hz, 1 H, Ar*H*), 7.52-7.46 (m, 2 H, Ar*H*), 7.44 (d, *J* = 8.0 Hz, 1 H, Ar*H*), 7.24 (bs, 1 H, CSN*H*), 7.07 (d, *J* = 8.1 Hz, 1 H, Ar*H*), 6.86-6.78 (m, 4 H, Het*H*), 6.05-6.04 (m, 2 H, Het*H*), 4.74 (d, *J* = 3.7 Hz, 2 H, ArCH_2NH), 4.50 (d, *J* = 4.5 Hz, 4 H, ArCH_2NH), 2.86-2.76 (m, 12 H, CH_2CH$_3$, NCH_3), 1.15-1.09 (m, 9 H, CH$_2$CH_3). ^{13}C-{^{1}H} NMR (125 MHz, DMSO-d_6): δ = 182.1, 160.3, 149.2, 144.1, 143.5, 132.6, 132.0, 131.0, 130.6, 128.5, 126.1, 125.4, 125.3, 124.2, 123.1, 121.3. 113.6, 110.6, 108.6, 44.9, 42.8, 37.0, 34.4, 22.7, 16.4, 16.3. MS (MALDI-TOF): *m/z*= 631.36, [*M*-S]$^{+}$ calcd. for $C_{38}H_{47}N_7O_2$ 631.87.

_N,N'_-(5-((3-(2-benzyl-1,3-dioxo-2,3-dihydro-1_H_-benzo[_de_]isoquinolin-6-yl)thioureido) methyl)-2,4,6-triethyl-1,3-phenylene)bis(methylene)bis(1_H_-pyrrole-2-carboxamide) (8)

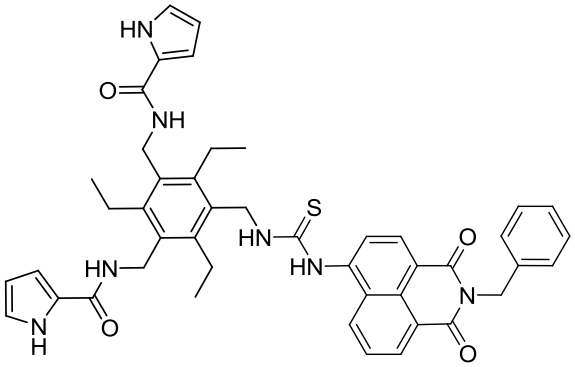

The 2-benzyl-6-isothiocyanato-1*H*-benzo[*de*]isoquinoline-1,3(2*H*)-dione (6.6 mg, 0.014 mmol) and **9** (5.2 mg, 0.014 mmol) were dissolved in freshly distilled THF in a vial. The vial was flushed with argon, screw-capped and covered with aluminum foil. The mixture was stirred at room temperature for 15 minutes. The solvent was then evaporated on a rotary evaporator and the residue was chromatographed on preparative TLC (silica, 2 mm, 20 × 20 cm, DCM/MeOH, 95 : 5 v/v, R_f = 0.26) and the product was isolated by extraction of the scraped silica layer into THF. Evaporation of THF afforded product **8** as a yellow solid (3.2 mg, 24 %). M.p. > 170 ^{o}C (dec.). ^{1}H NMR (500 MHz, DMSO-d_6): δ = 11.51-11.43 (m, 2 H, HetN*H*), 10.14-10.06 (m, 1 H, CSN*H*), 8.54-8.46 (m, 4 H, Ar*H*), 8.36 (m, 1 H, CSN*H*), 7.90-7.87 (m, 3 H, Het*H*), 7.35-7.21 (comp, 5 H, Ar*H*), 6.85-6.82 (comp, 4 H, Het*H*), 6.05-6.03 (m, 2 H, Het*H*), 5.25 (s, 2 H, PhCH_2), 4.79 (d, J = 3.5 Hz, 2 H, ArCH_2NH), 4.54 (d, J = 4.4 Hz, 4 H, ArCH_2NH), 2.89-2-82 (comp, 6 H, CH_2CH_3), 1.27-1.06 (m, 12 H, CH_2CH_3). ^{13}C-{^{1}H} NMR (125 MHz, DMSO-d_6): δ = 180.6, 163.6, 163.0, 160.3, 144.3, 143.5, 142.0, 137.4, 132.8, 131.6, 131.2, 128.8, 128.5, 128.4, 127.5, 127.1, 126.8, 126.1, 125.7, 122.3, 121.9, 121.3, 117.5, 110.6, 108.6, 42.8, 42.7, 36.9, 22.8, 22.7, 16.4, 16.3. MS (MALDI-TOF): *m/z*= 802.43, $[M+Na]^+$ calcd. for $C_{45}H_{45}N_7NaO_4S$ 802.32.

NMR Spectra

Sensor 4. ^{1}H NMR

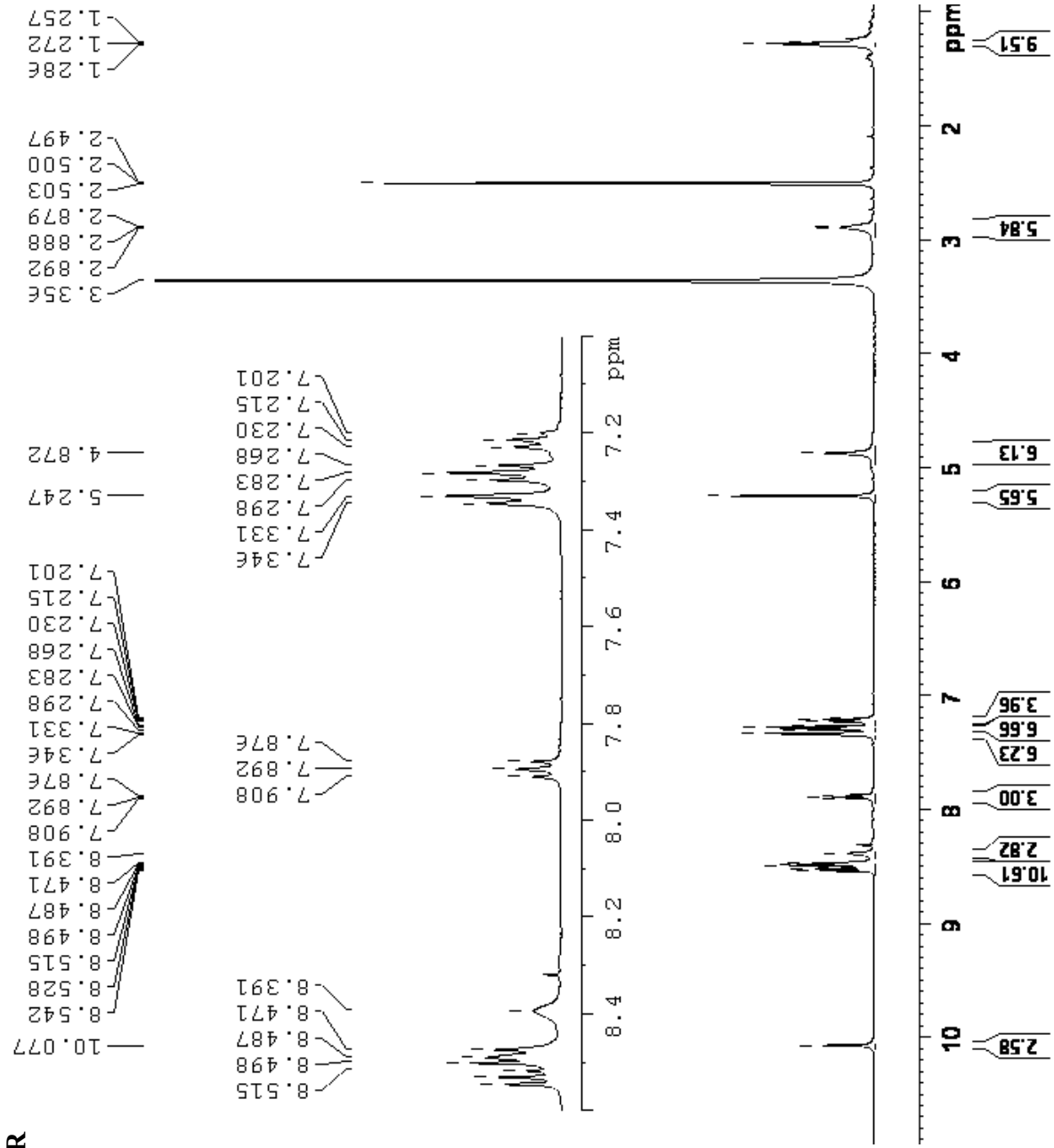

Sensor 4. ^{13}C NMR

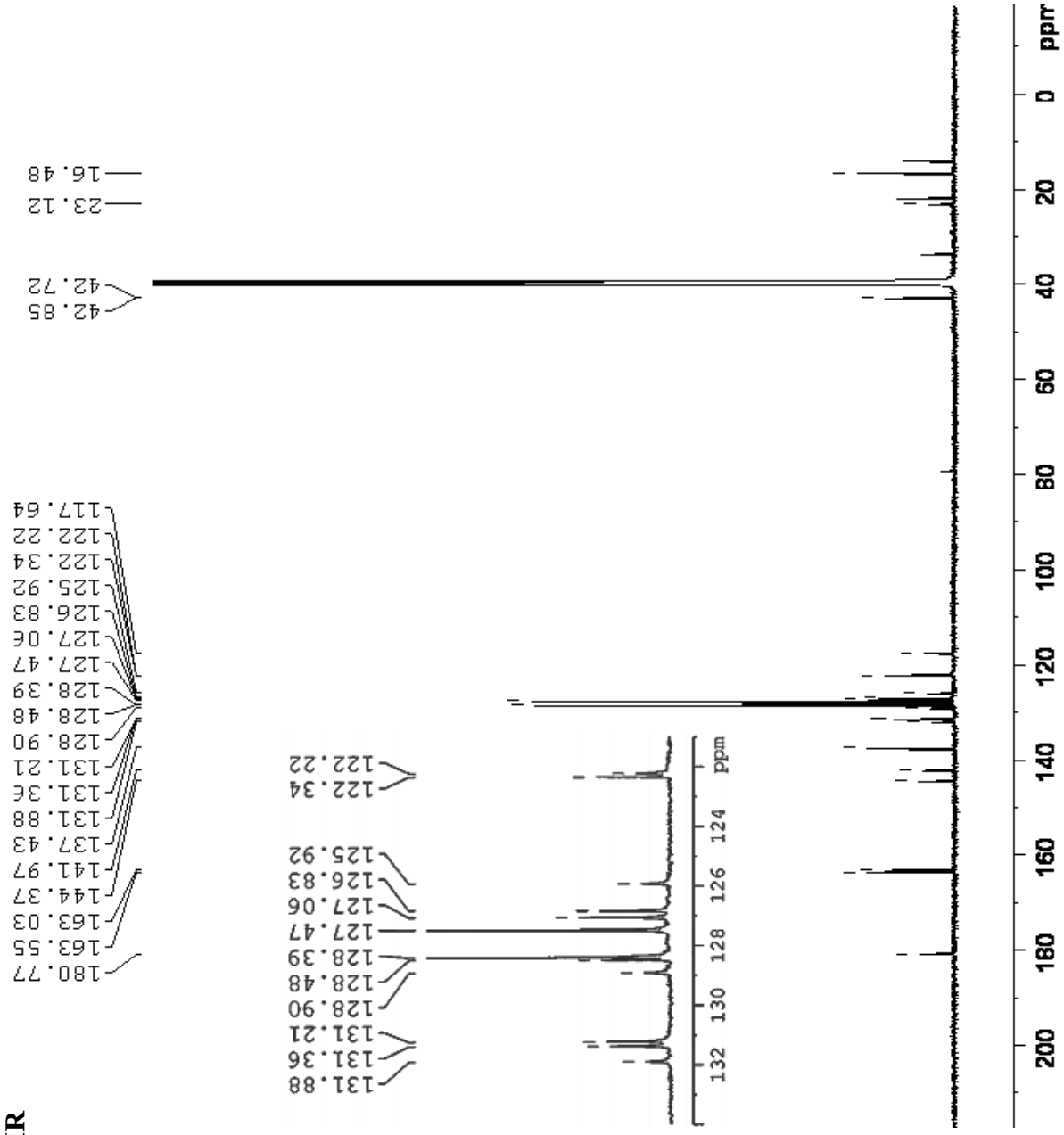

Sensor 5. ^{1}H NMR

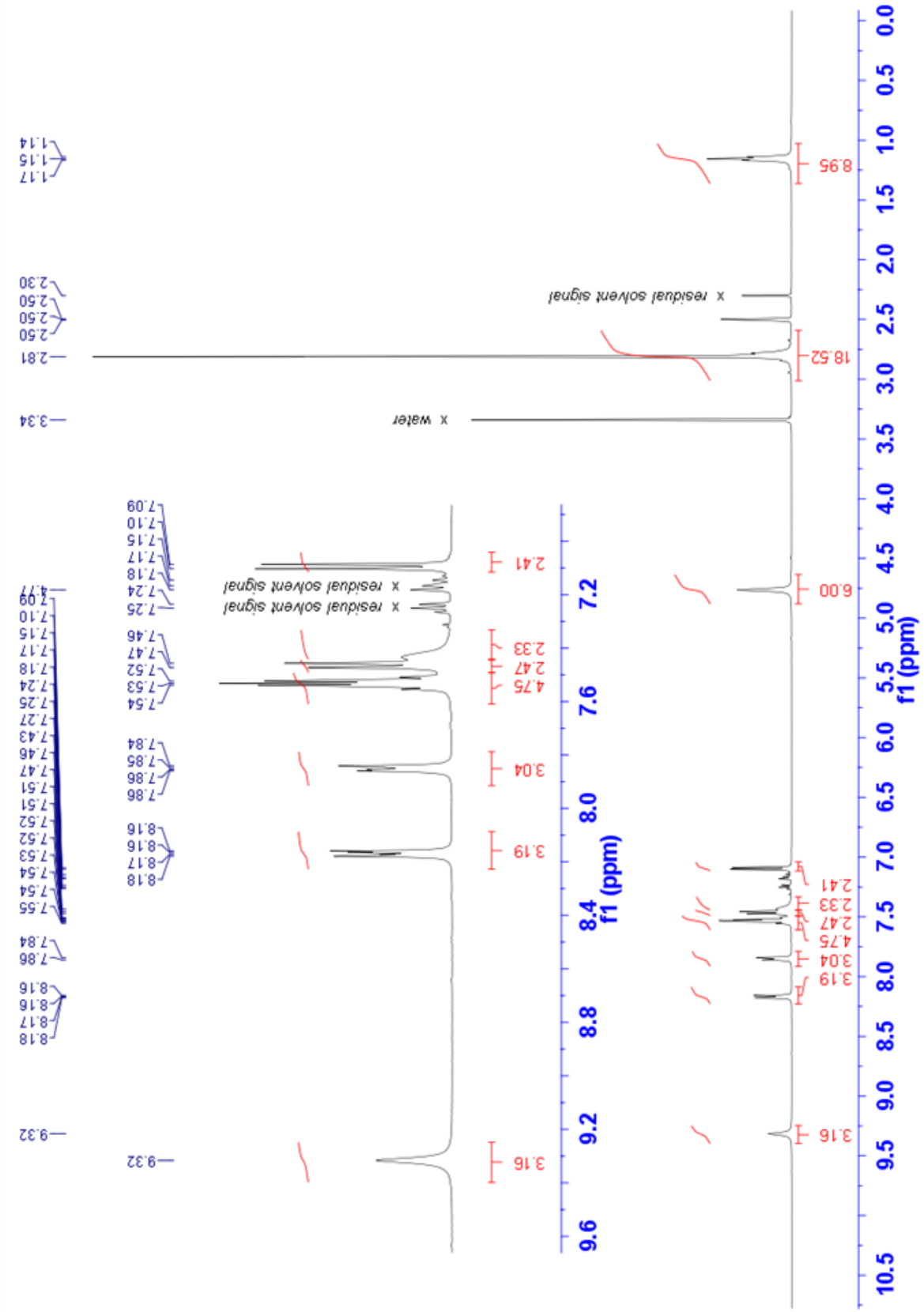

Sensor 5. ^{13}C NMR

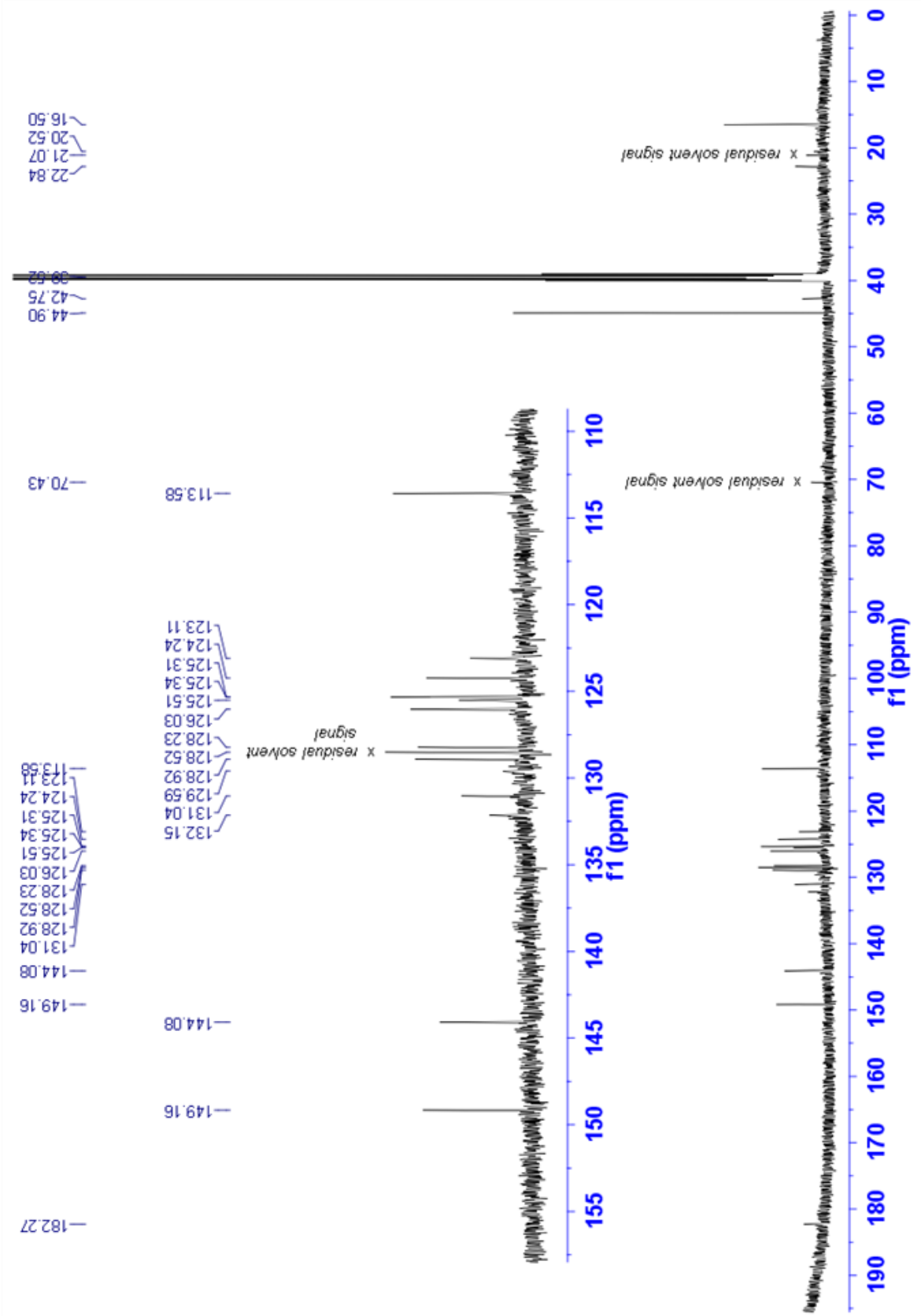

Sensor 7. ^{1}H NMR

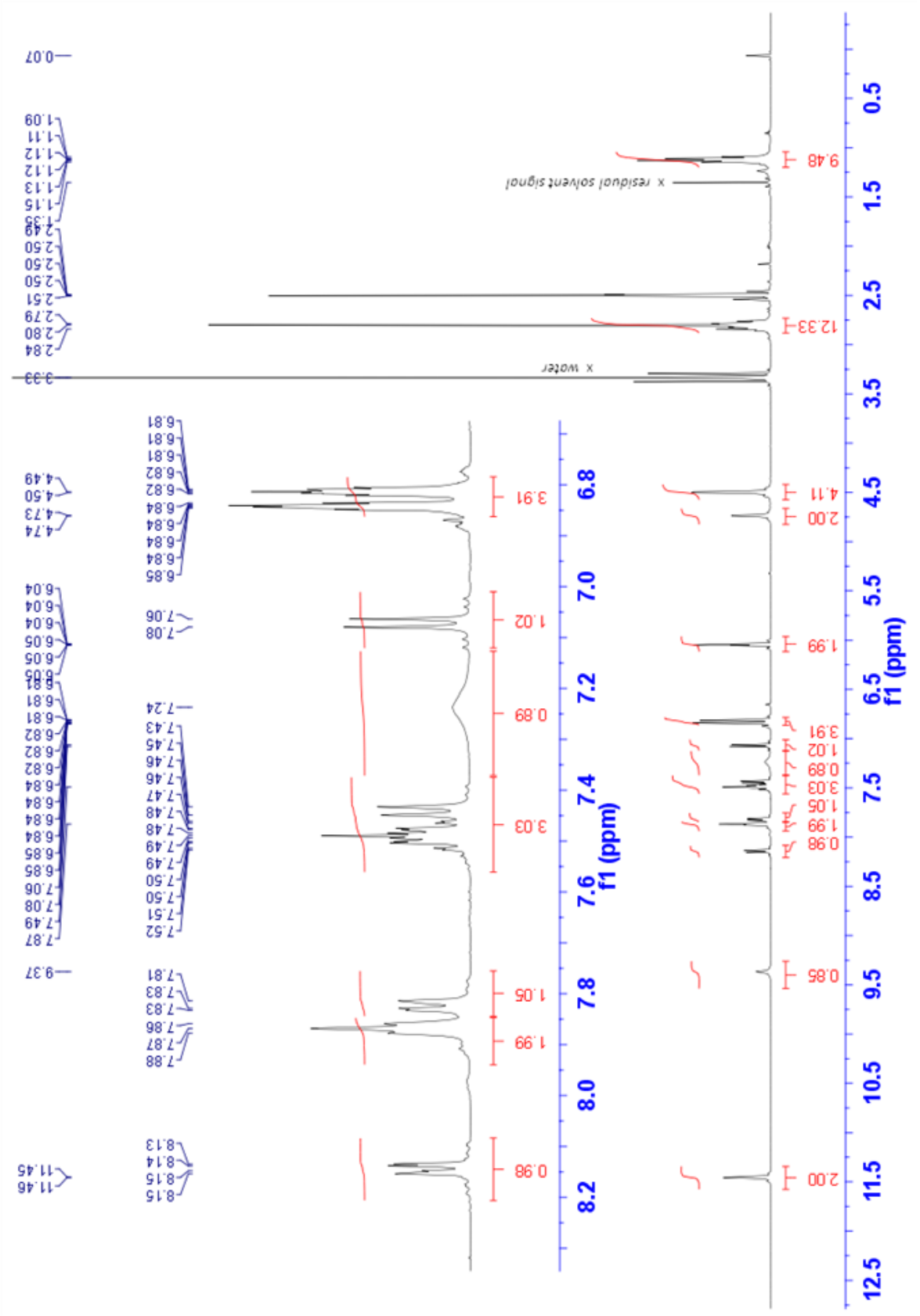

Sensor 7. ^{13}C NMR

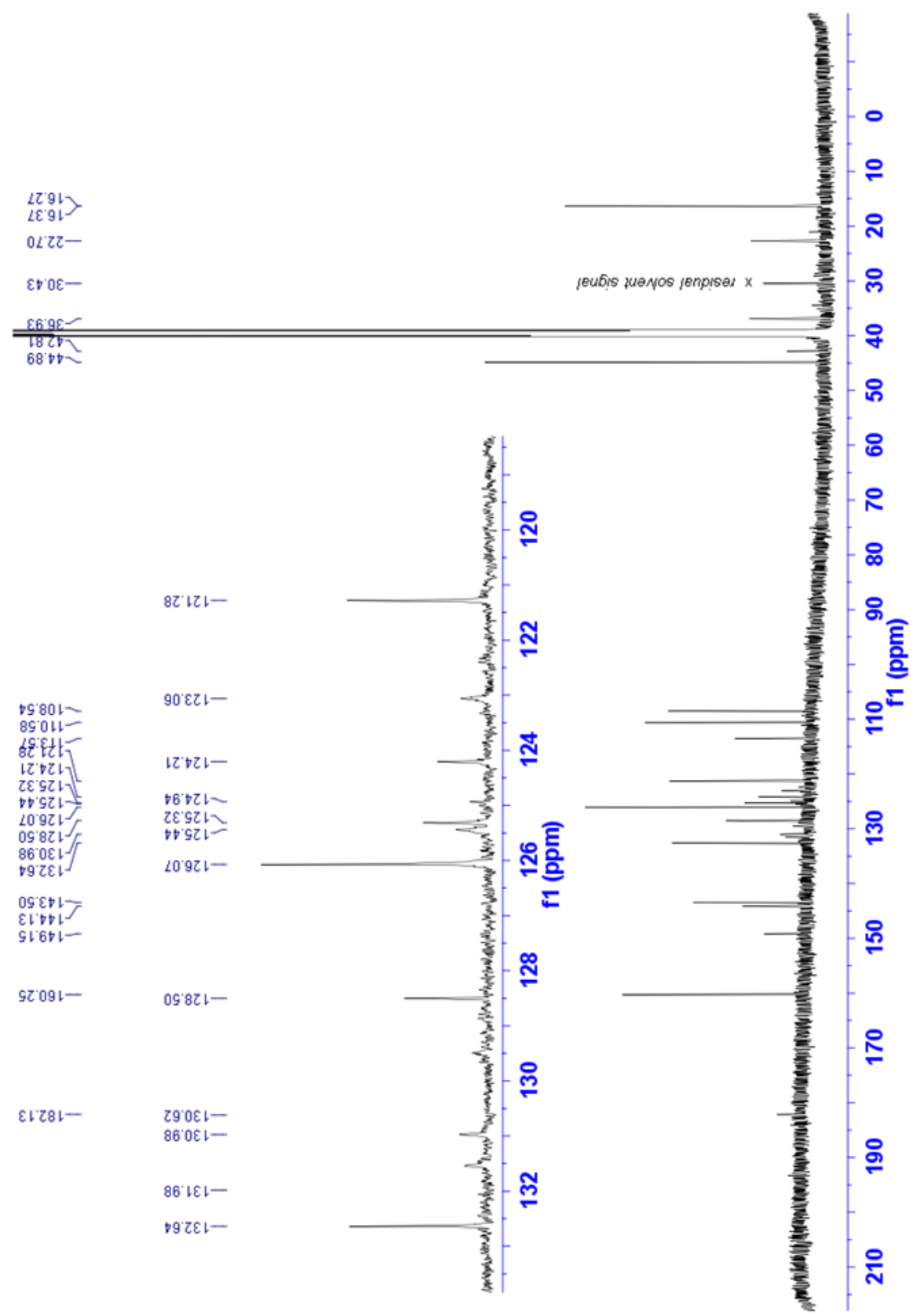

Sensor 8. ^{1}H NMR

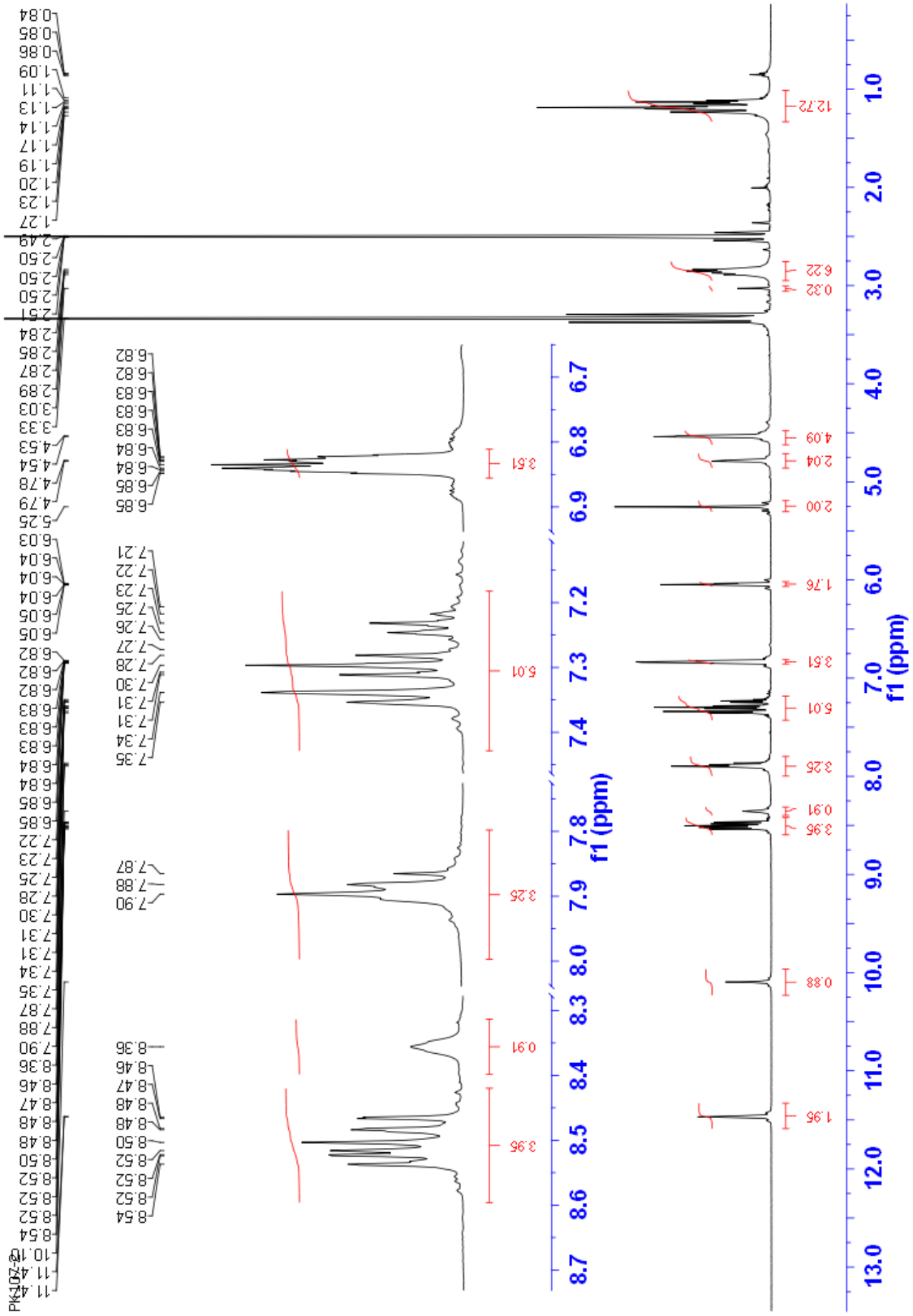

Sensor 8. ^{13}C NMR

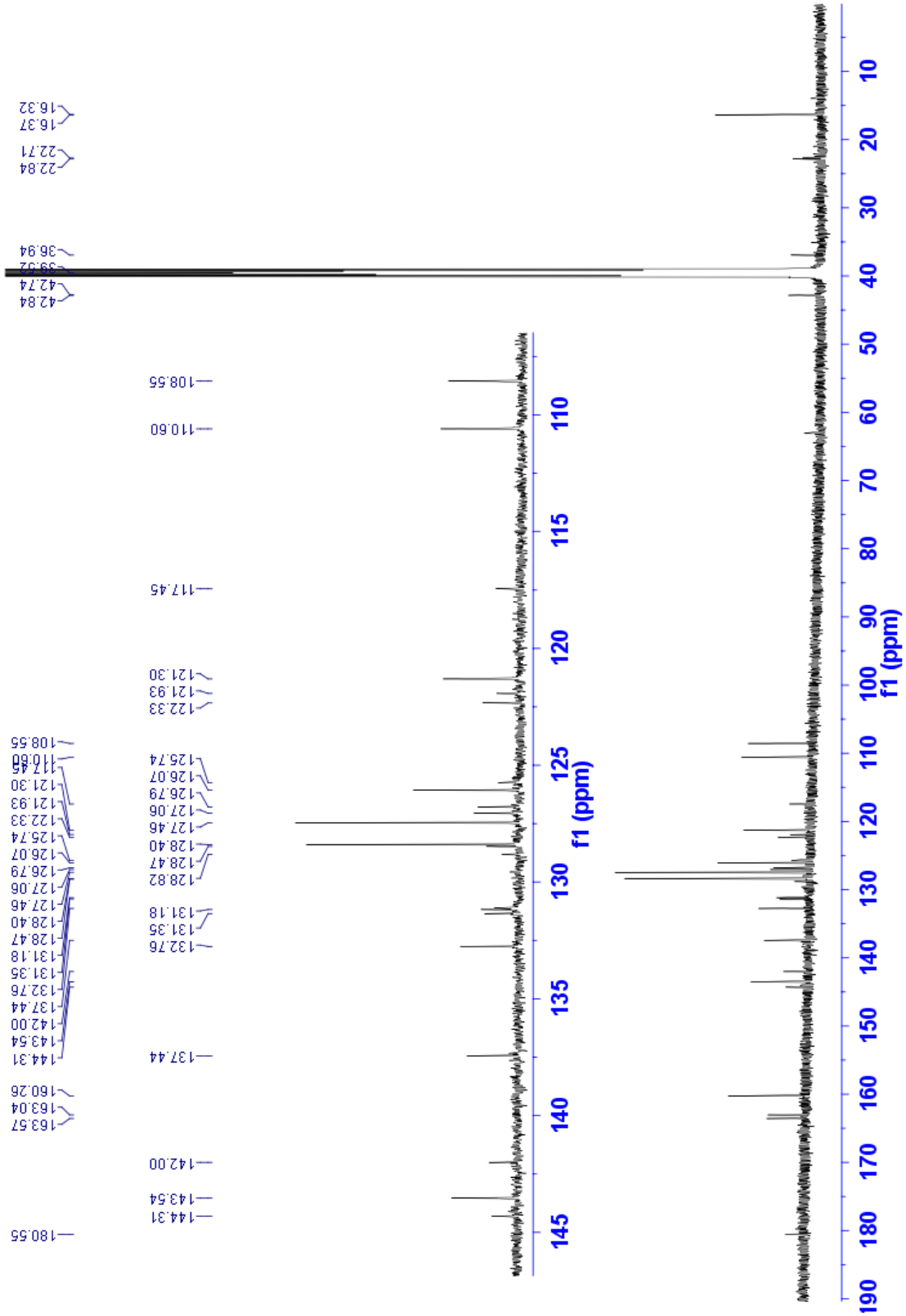

9. ^{1}H NMR

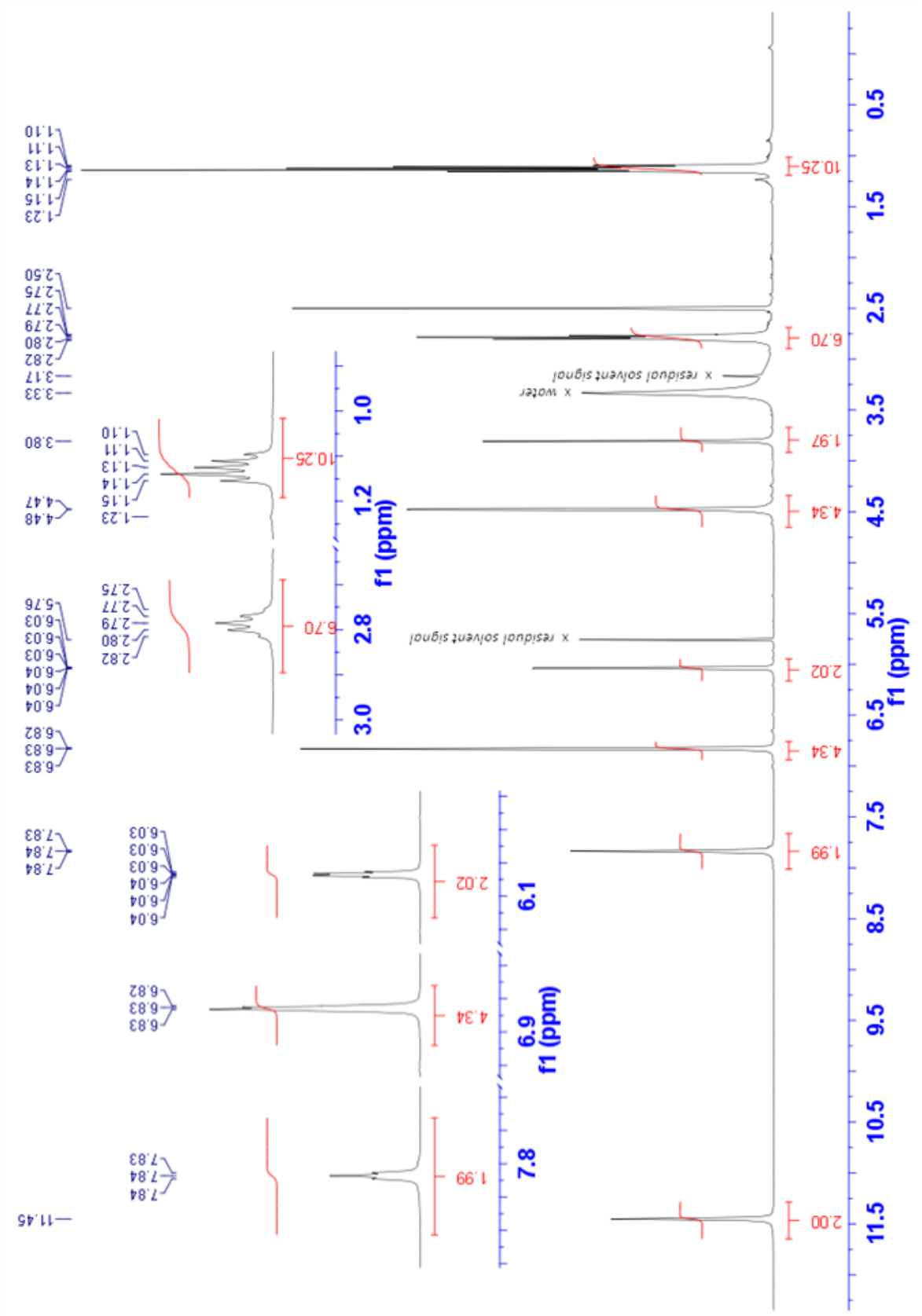

9. ^{13}C NMR

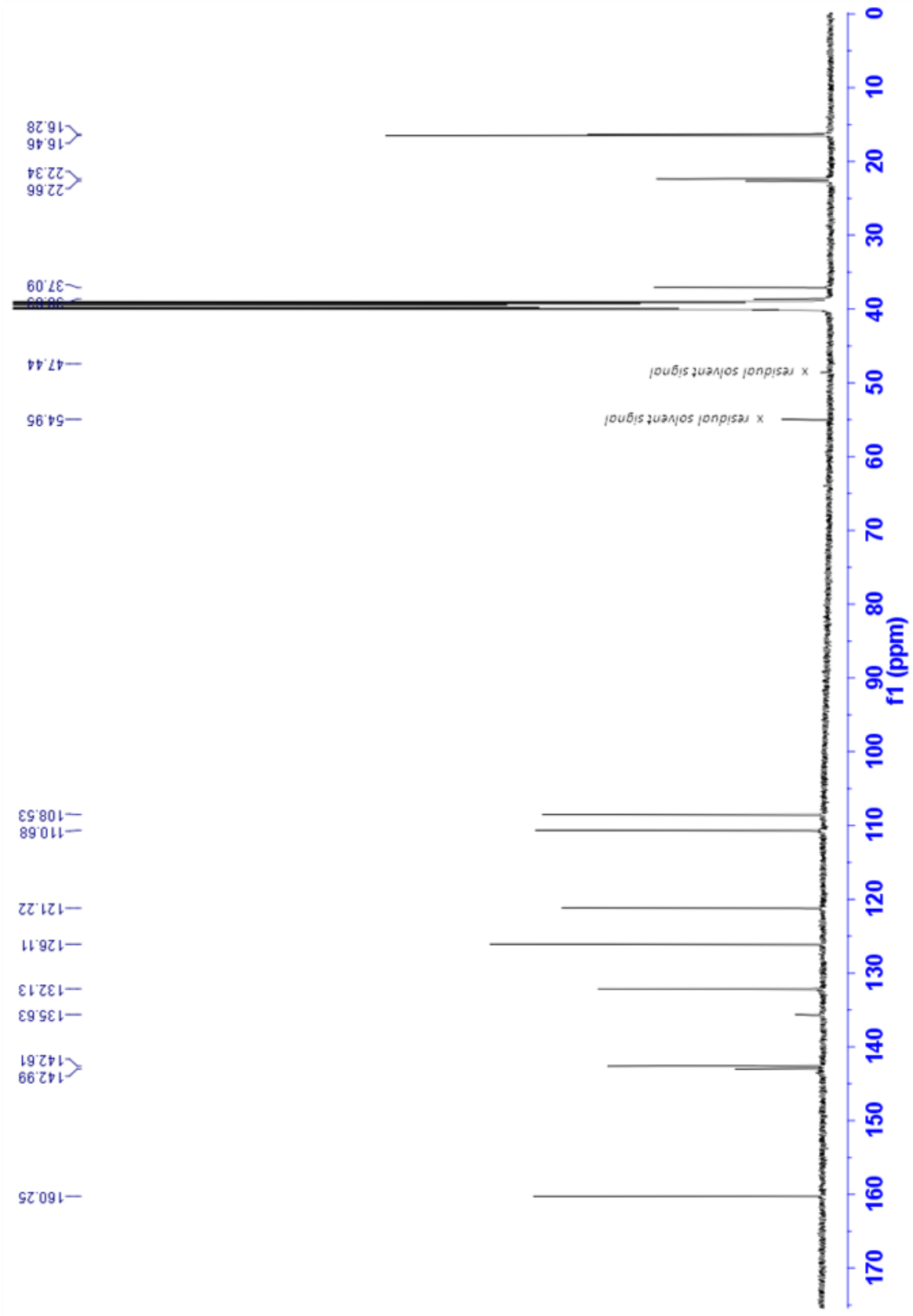
160.25
142.99
142.61
135.63
132.13
126.11
121.22
110.68
108.53
54.95
47.44
37.09
22.66
22.34
16.46
16.28
x residual solvent signal
x residual solvent signal
f1 (ppm)

X-ray structural analysis

The data were collected on a Nonius Kappa CCD diffractometer using a graphite monochromatized Mo-K_α radiation (λ = 0.71075 Å) at 153 K using an Oxford Cryostream low temperature device. Data reduction was performed using DENZO-SMN.[3] The structure was solved by direct methods using SIR97[4] and refined by full-matrix least-squares on F^2 with anisotropic displacement parameters for the non-H atoms using SHELXL-97.[5] The hydrogen atoms on carbon were calculated in ideal positions with isotropic displacement parameters set to 1.2xUeq of the attached atom (1.5xUeq for methyl hydrogen atoms). The function, $\Sigma w(|F_o|^2 - |F_c|^2)^2$, was minimized, where $w = 1/[(\sigma(F_o))^2 + (0.0499*P)^2 + (1.0626*P)]$ and $P = (|F_o|^2 + 2|F_c|^2)/3$. Neutral atom scattering factors and values used to calculate the linear absorption coefficient are from the *International Tables for X-ray Crystallography* (1992).[6] All figures were generated using Mercury from CCDC.

Table S1 X-ray structural analysis details for the crystals obtained with sensor **2**, **3** and **5**

compound reference	**2**·diox$_6$	**3**·3H$_2$PO$_4$	**5**
crystal system	Triclinic	Hexagonal	Triclinic
radiation type	MoKα	MoKα	MoKα
wavelength (Å)	0.71075	0.71075	0.71075
a (Å)	12.595	20.6054(3)	15.1253(2)
b (Å)	13.891	20.6054(3)	18.3340(2)
c (Å)	15.904	13.2836(2)	19.6654(2)
α (°)	76.09	90.00	99.2540(10)
β (°)	86.26	90.00	97.6060(10)
γ (°)	89.20	120.00	90.4190(10)
V (Å^3)	2695.2	4884.37(12)	5332.75(11)
T (K)	293(2)	153(2)	153(2)
space group	*P*,-1	*P*63	*P*,-1
Z	1	2	4
μ (mm^{-1})	0.096	0.184	0.223
Theta range (°)	2.02–27.12	2.28–27.46	1.79–27.50
No. of reflections measured	7210	14881	37374
No. of independent reflections	7210	7463	24321
R_{int}	0.0000	0.0370	0.0234
R_1 ($I > 2\sigma(I)$)	0.0867	0.0472	0.0751
$wR(F^2)$ ($I > 2\sigma(I)$)	0.1405	0.1037	0.1685
R_1 (all data)	0.1731	0.0801	0.1238
$wR(F^2)$ (all data)	0.1602	0.1170	0.1762
GOF on F^2	1.435	1.055	2.633
Δr_{max}, Δr_{min} (e Å^{-3})	0.549, –0.332	0.422, –0.301	1.290, –2.551
Δr (rms) (e Å^{-3})	0.049	0.043	0.082

2·diox_6: A crystal suitable for single-crystal X-ray diffractometric analysis was obtained by slow evaporation from a dioxane solution. The unit cell contains two molecules of receptor **2** and 12 molecules of co-crystallized dioxane. One of the dioxane molecules resides on the inversion centre. **3**·3$\mathbf{H_2PO_4}$: Crystals of **3** in presence of tetrabutylammonium dihydrogenphosphate suitable for X-ray analysis were grown from acetone solution. The unit cell of the hexagonal crystal contains two molecules of **3**, six dihydrogenphospate anions and 6 tetrabutylammonium cations. The molecule resides around a crystallographic three-fold rotation axis at 2/3, 1/3, z. **5** Crystallizes in the triclinic system and crystals suitable for X-ray diffraction were obtained by slow evaporation of an acetone solution.

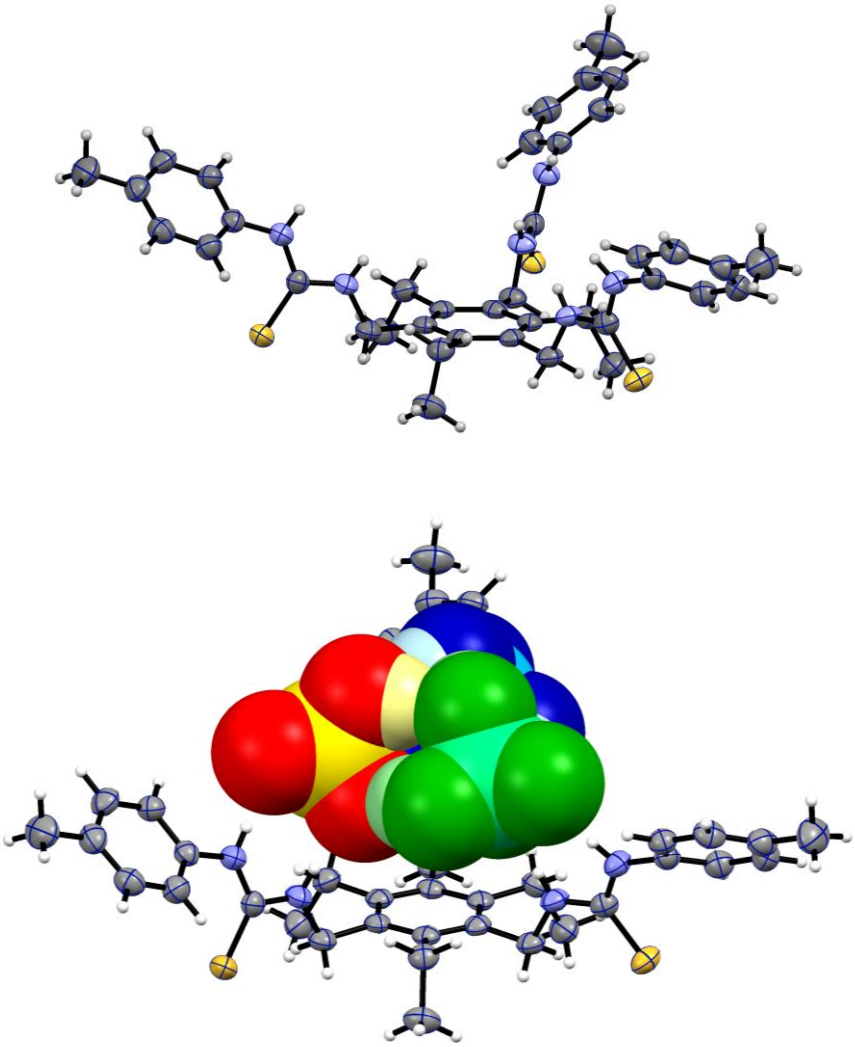

Fig. S1 Two views of [**3**·3$\mathbf{H_2PO_4^-}$] showing displacement ellipsoids scaled to the 50% probability level. **Top:** 3$\mathbf{H_2PO_4^-}$ cluster has been removed for clarity. In the bottom panel the three $H_2PO_4^-$ anions have been colored differently.

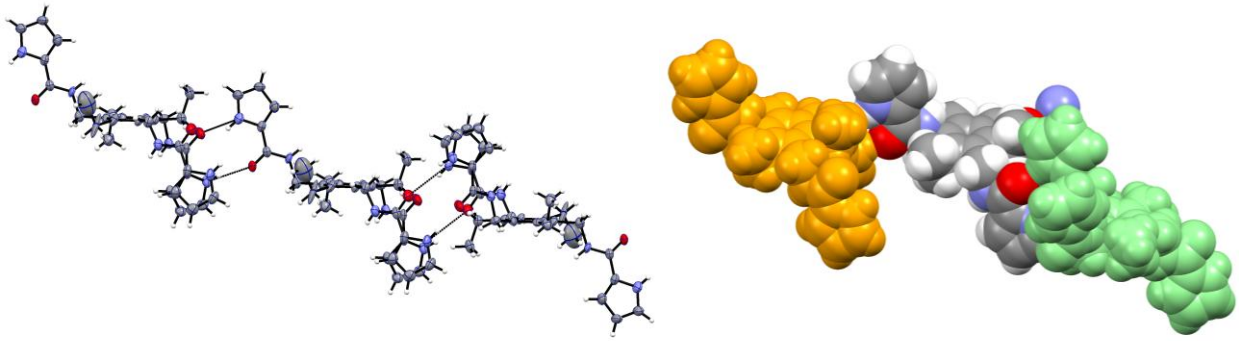

Fig. S2 View of the up-down arrangement of the arms of **2**. Interaction of neighboring molecules of **2** is highlighted. The dashed line represent the hydrogen bonds formed between the pyrrole N-H and the amidic C=O.

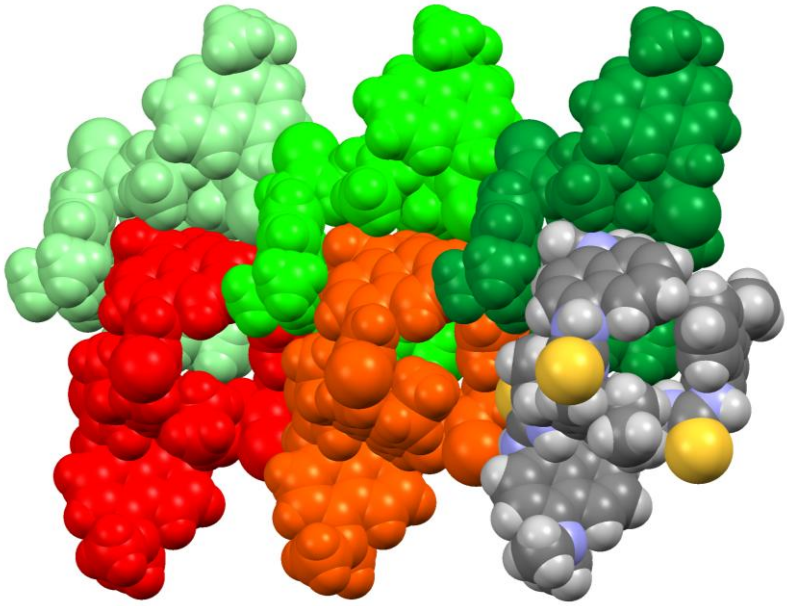

Fig. S3 The spacefill model of **5** shows the closely interdigitated structure of the crystal. The sensor molecules maximize the number of interactions by adopting an up-down conformation of the arms.

Solution Behavior by Variable-Temperature NMR

Variable-temperature ^{1}H NMR spectra of **2**:$Bu_4NH_2PO_4$ = 1:1 were recorded in a mixture of CD_3CN:acetone-d_6:DMSO-d_6 = 10:1:0.5 due to the low freezing point of this solvent. As the temperature is reduced, the amidopyrrole and methylene signals display a little shifting and some broadening, although no peak splitting occurs, probably due to the "locking" of the conformation upon complexation with phosphate anion.

Fig. S4 VT-NMR of the receptor **2** in the presence of $H_2PO_4^-$.

Examples of NMR titrations

In a typical titration procedure, 1.0 ml of sensor solution (**[2]** = **[3] =** 1.0×10^{-2} M) was placed in a NMR tube. The NMR spectrum was recorded in the absence of anion at room temperature. Then NMR spectra were repeatedly acquired after addition of 1 µL aliquots of anion solution. The stock solutions of anions contained the same concentration of sensor as the initial solution titrated. Some of the NMR isotherms display a slight signoidal dependence, which is presumed to be due to the sensor self-association at high NMR concentrations.

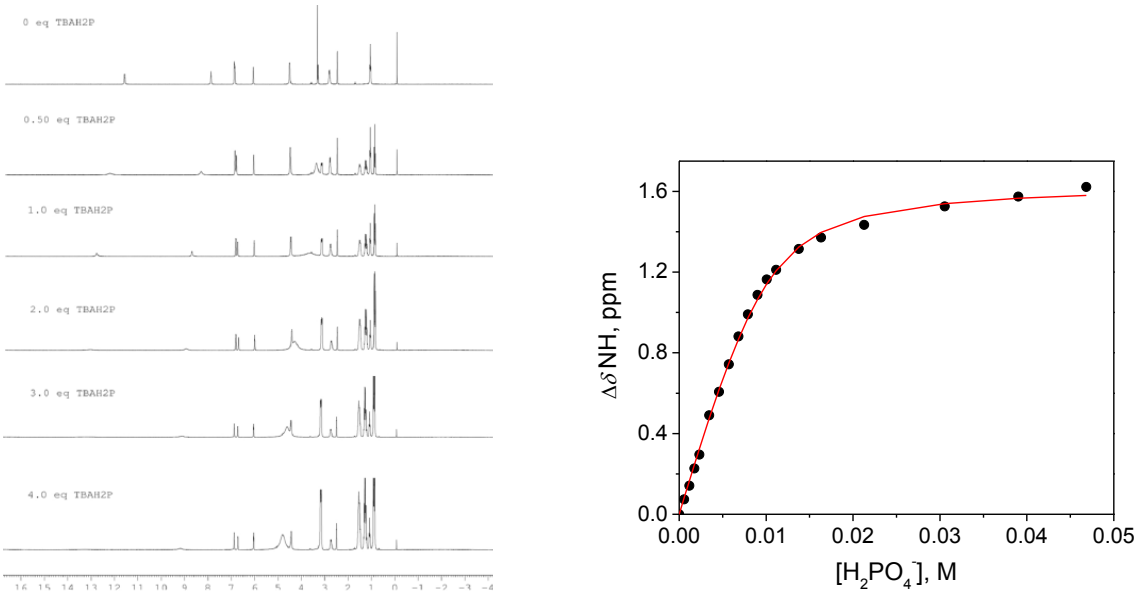

Fig. S5 ^{1}H NMR spectra of **2** (2.0×10^{-2} M) titrated with $H_2PO_4^-$ (0.5, 1.0, 2.0, 3.0, and 4.0 eq.).

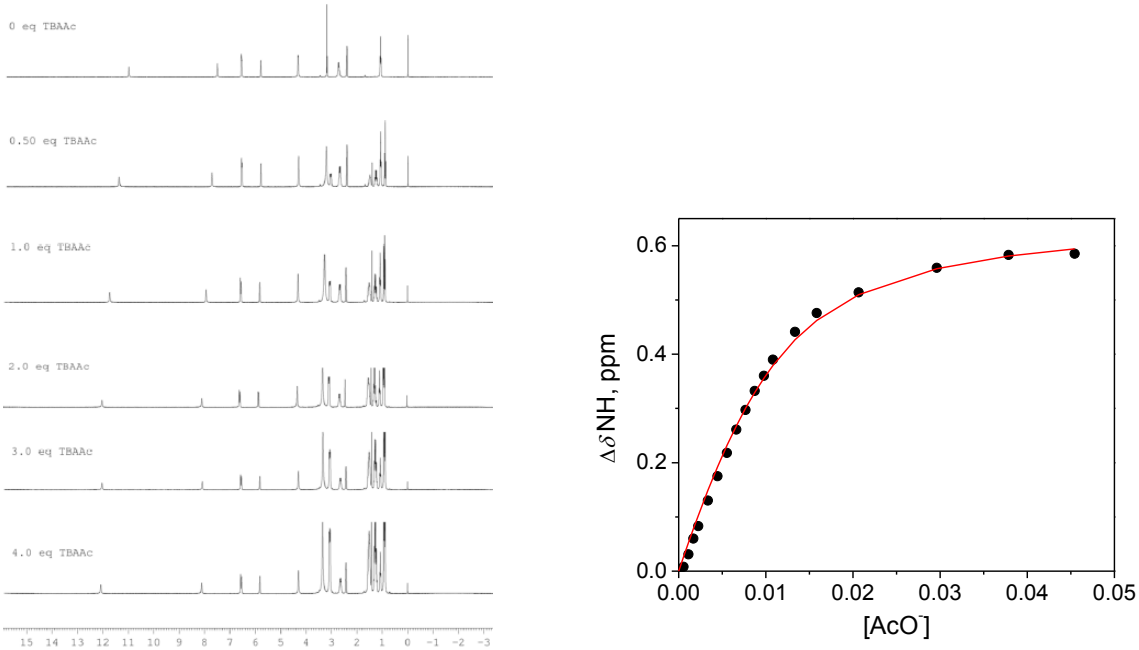

Fig. S6 ^{1}H NMR spectra of **2** (2.0×10^{-2} M) titrated with AcO^- (0.5, 1.0, 2.0, 3.0, and 4.0 eq.).

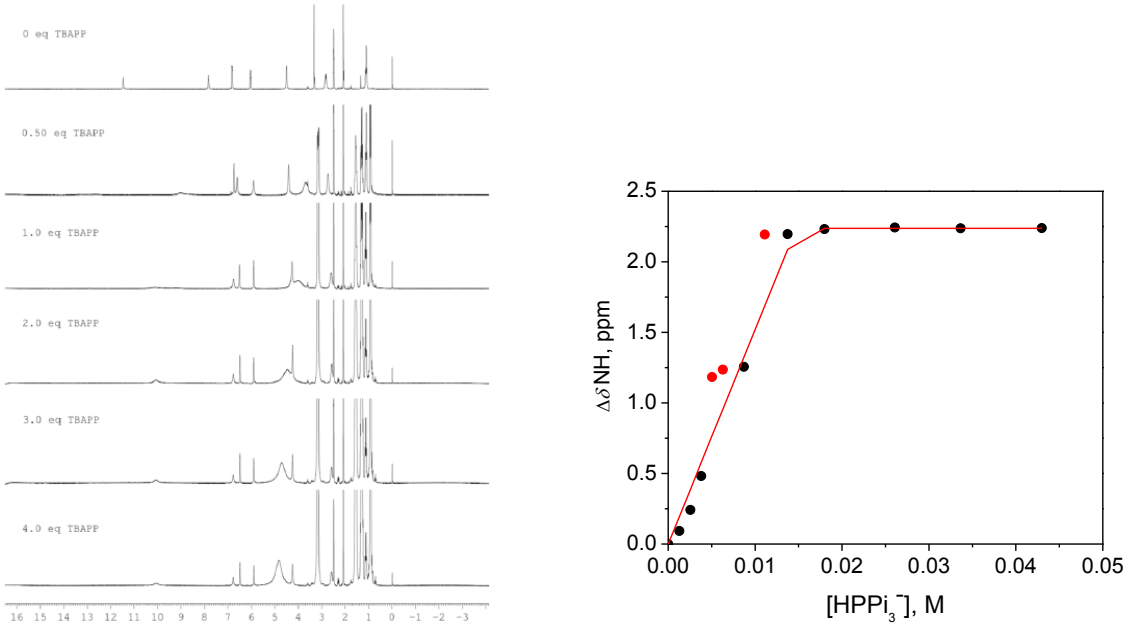

Fig. S7 ^{1}H NMR spectra of **2** (2.0×10^{-2} M) titrated with $HPPi^{3-}$ (0.5, 1.0, 2.0, 3.0, and 4.0 eq.).

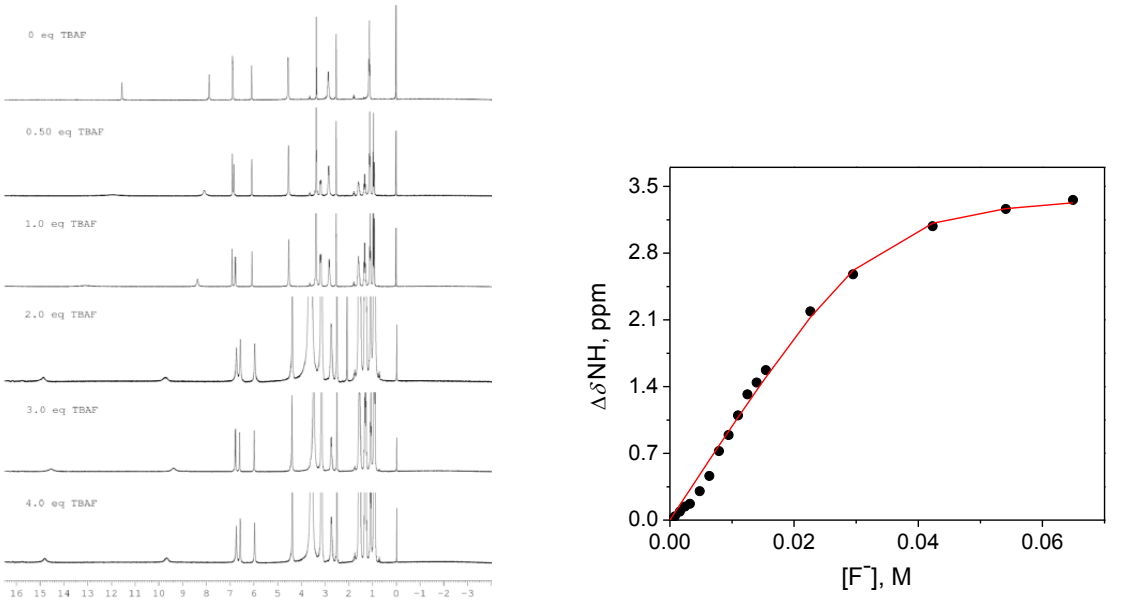

Fig. S8 ^{1}H NMR spectra of **2** (2.0×10^{-2} M) titrated with F^{-} (0.5, 1.0, 2.0, 3.0, and 4.0 eq.).

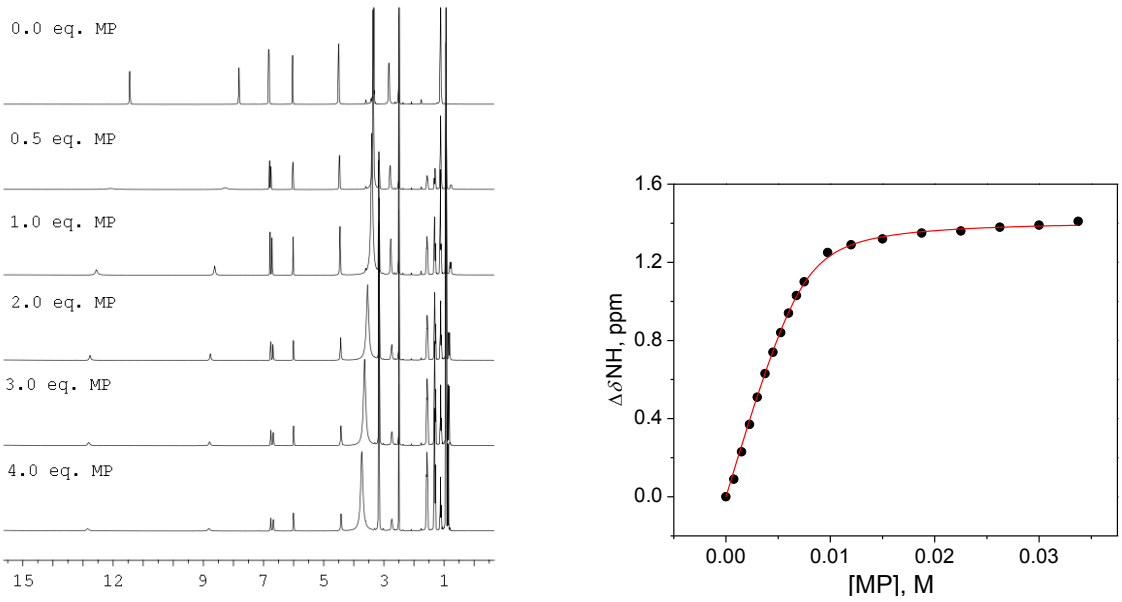

Fig. S9 ^{1}H NMR spectra of **2** (2.0×10^{-2} M) titrated with MP (0.5, 1.0, 2.0, 3.0, and 4.0 eq.).

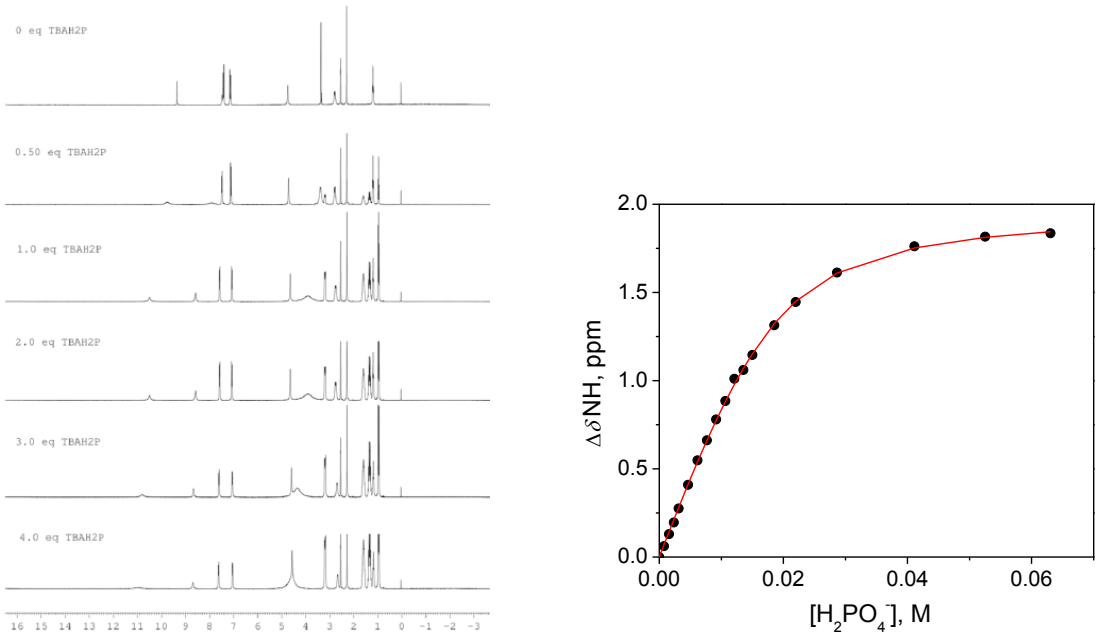

Fig. S10 ^{1}H NMR spectra of **3** (2.0×10^{-2} M) titrated with $H_2PO_4^-$ (0.5, 1.0, 2.0, 3.0, and 4.0 eq.).

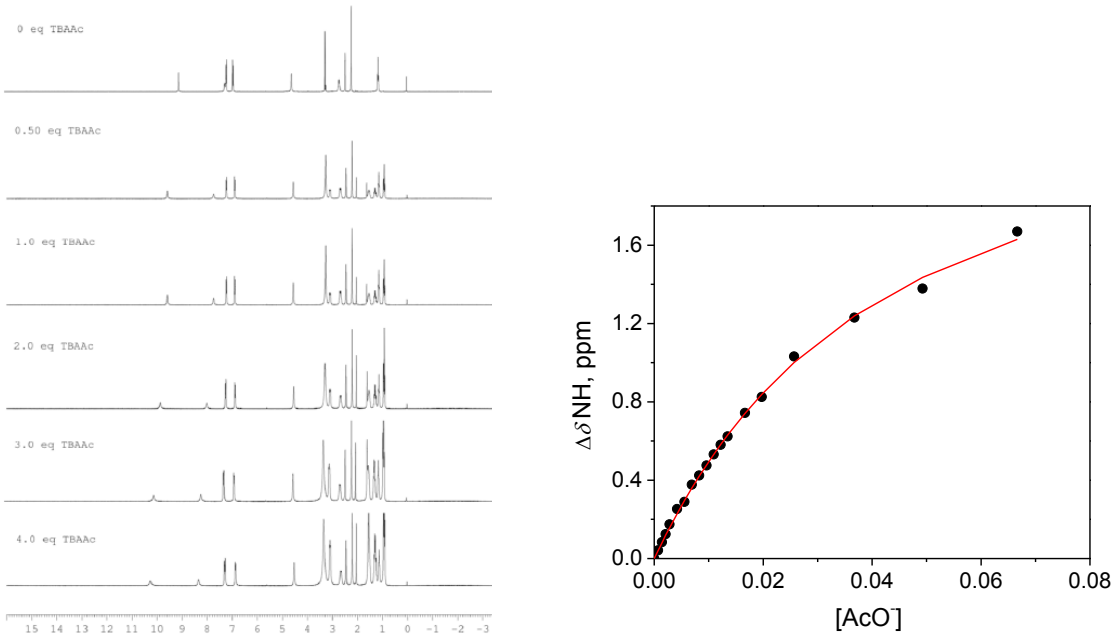

Fig. S11 ^{1}H NMR spectra of **3** (2.0×10^{-2} M) titrated with AcO^{-} (0.5, 1.0, 2.0, 3.0, and 4.0 eq.).

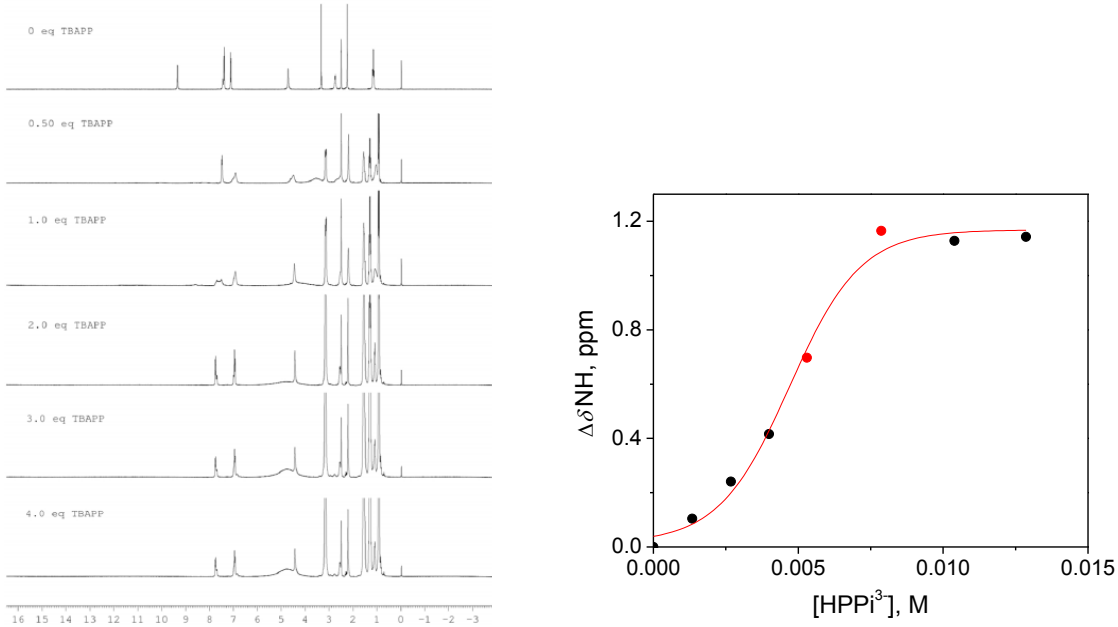

Fig. S12 ^{1}H NMR spectra of **3** (2.0×10^{-2} M) titrated with $HPPi^{3-}$ (0.5, 1.0, 2.0, 3.0, and 4.0 eq.).

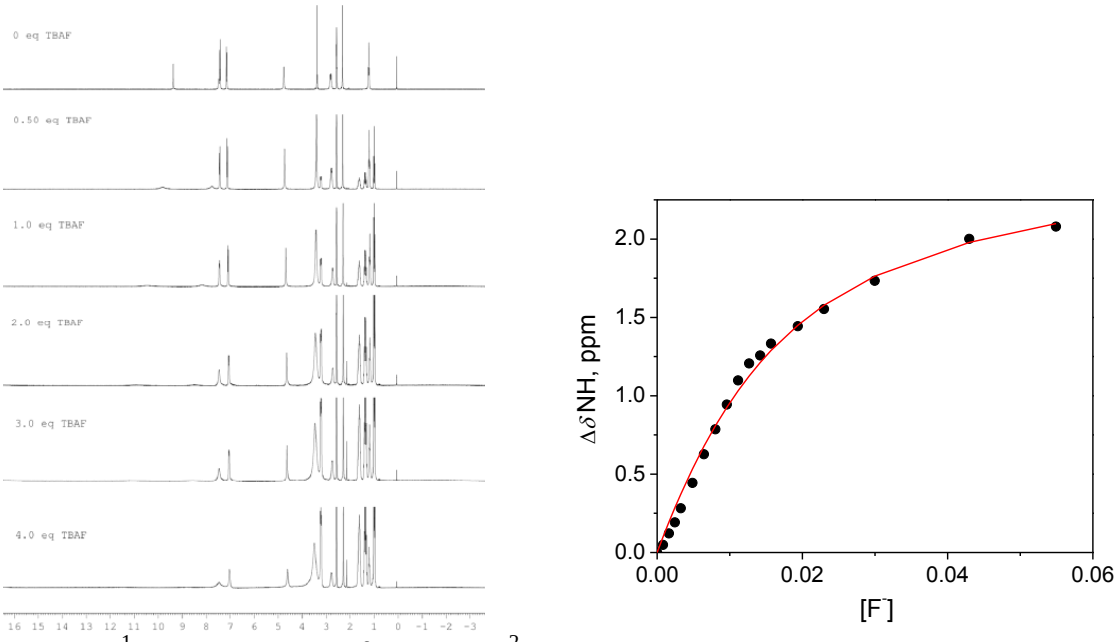

Fig. S13 ^{1}H NMR spectra of **3** (2.0×10^{-2} M) titrated with F^- (0.5, 1.0, 2.0, 3.0, and 4.0 eq.).

MALDI and Electrospray mass-spectrometric studies of sensor-anion complexes

In a typical procedure 1.0 μL of 1.0×10^{-5} M solution of sensor **2** with an excess of a corresponding anion in acetone was spotted onto the target using a syringe. The MALDI-TOF spectrum was recorded in the negative mode.

In a typical procedure, 10.0 μL of 1.0×10^{-5} M solutions of **2** or **3** with an excess of a corresponding anion in 50-90% acetonitrile were introduced into the ionization chamber using a syringe. The ESI spectrum was recorded at room temperature using positive or negative detection mode.

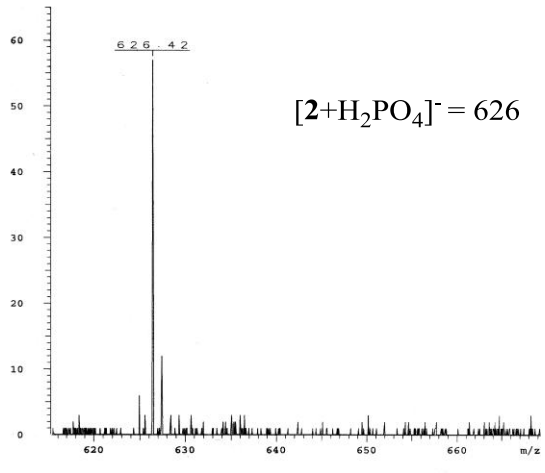

$[\mathbf{2}+H_2PO_4]^- = 626$

Fig. S14 MALDI-TOF mass spectrum of **2**•dihydrogenphoshate complex.

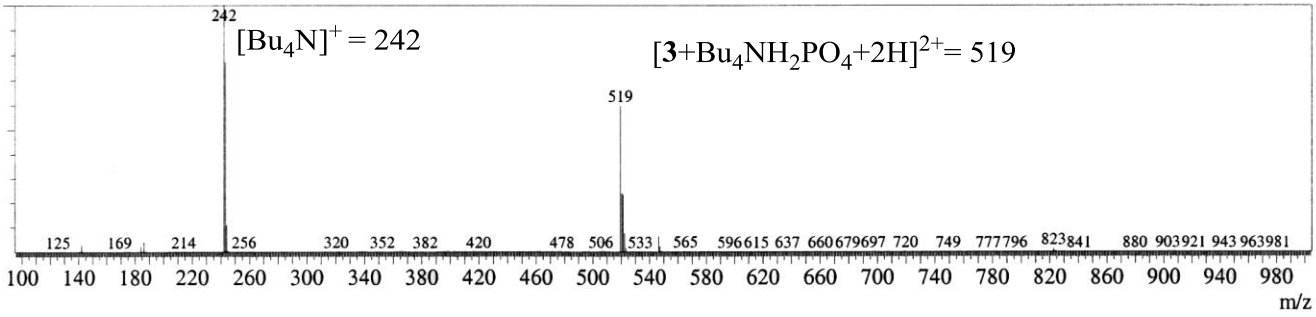

Fig. S15 ESI mass spectrum of **3**•dihydrogenphosphate complex.

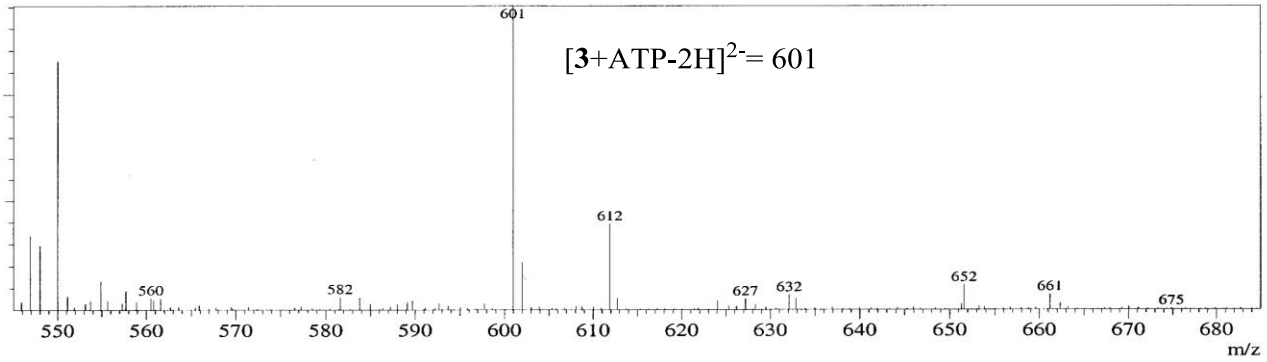

Fig. S16 ESI mass spectrum of **3**•ATP complex.

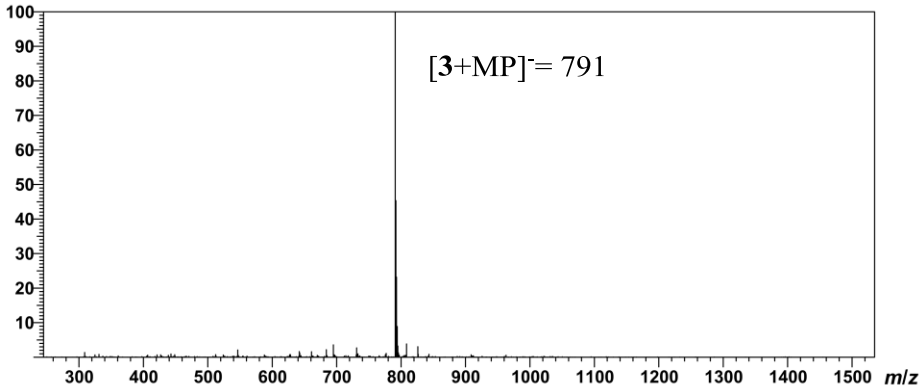

Fig. 17 ESI mass spectrum (negative mode) of the complex of **3**•MP in acetonitrile.

Job-Plot Experiments

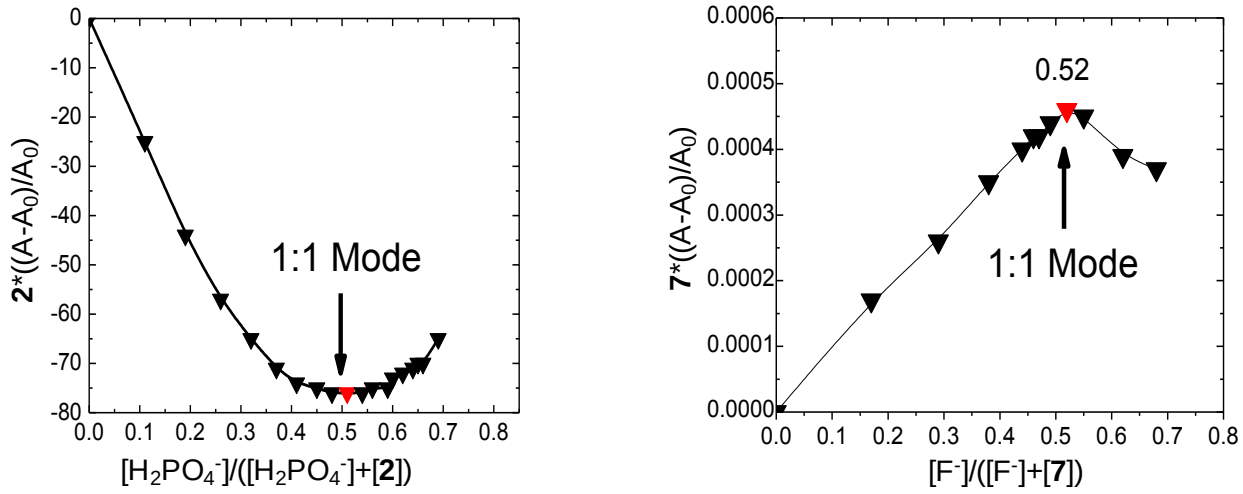

Fig. S18 UV-Vis titrations of **2** with $H_2PO_4^-$ (left) and **7** with F^- (right).

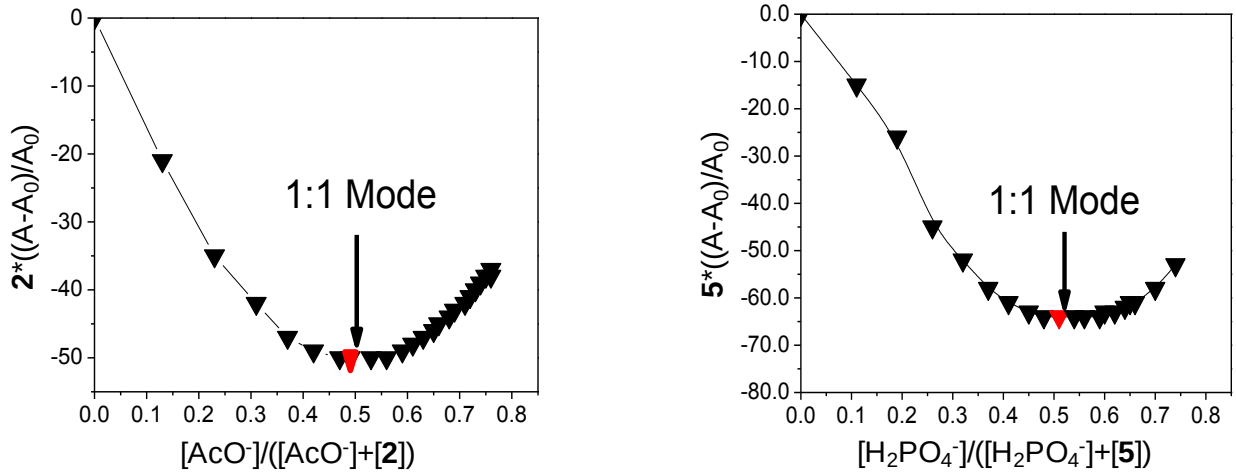

Fig. S19 UV-Vis titrations of **2** with AcO^- (left) and **5** with $H_2PO_4^-$ (right).

Photophysical properties and fluorimetric titrations

In a typical titration procedure, 3.0 ml of a sensor solution were placed in a 1 cm fluorescence cell. The fluorescence spectrum was recorded in the absence of an anion at room temperature. Then the emission spectra were repeatedly acquired after addition of 1-2 μL aliquots of anion solution. The stock solutions of anions contained the same concentration of sensor as the initial solution titrated. All sensors were excited at the isosbestic point of their absorption or at the point where no change in absorption is observed. The photophysical properties of **5-7** were reported previously.[2]

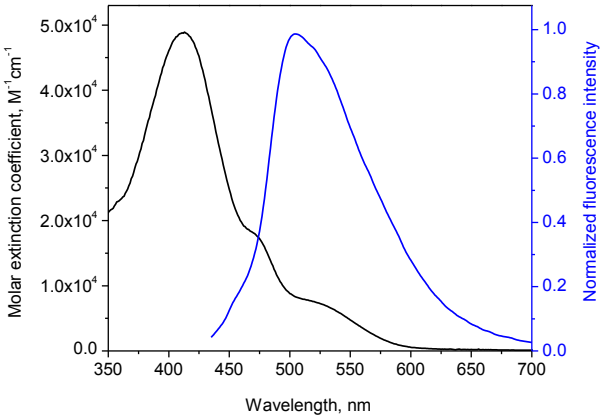

φ = 10.4 ± 1 %; τ_1 = 4.5 ns, τ_2 = 23.5 ns

Fig. S20 Absorption and emission spectra of **4** in DMSO. λ_{ex} = 400 nm.

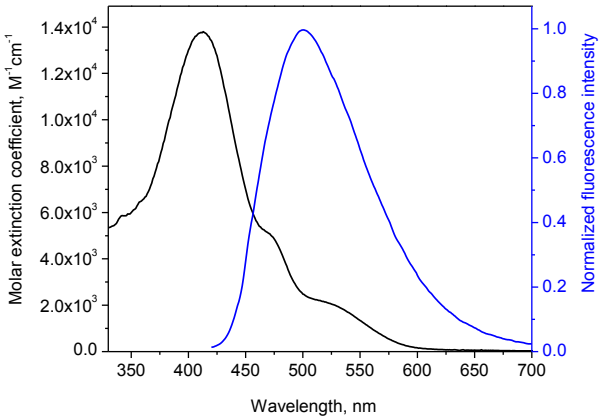

φ = 11.9 ± 1 %; τ_1 = 6.5 ns, τ_2 = 21.9 ns

Fig. S21 Absorption and emission spectra of **8** in DMSO. λ_{ex} = 400 nm.

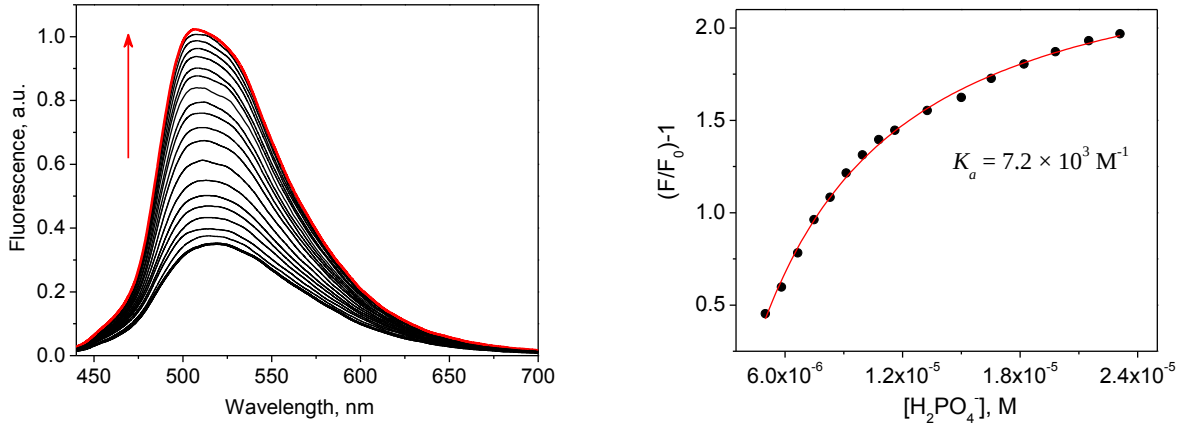

Fig. S22 Fluorescence spectra of **4** (10 μM) upon the addition of $H_2PO_4^-$ in DMSO. λ_{ex} = 400 nm. [$H_2PO_4^-$] = 0 – 25 μM.

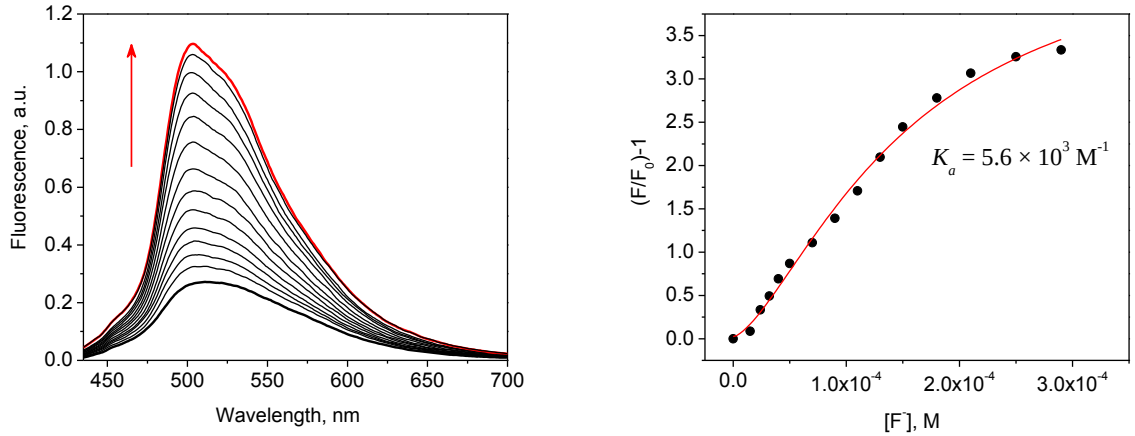

Fig. S23 Fluorescence spectra of **4** (10 μM) upon the addition of F^- in DMSO. λ_{ex} = 400 nm. [F^-] = 0 – 0.30 mM.

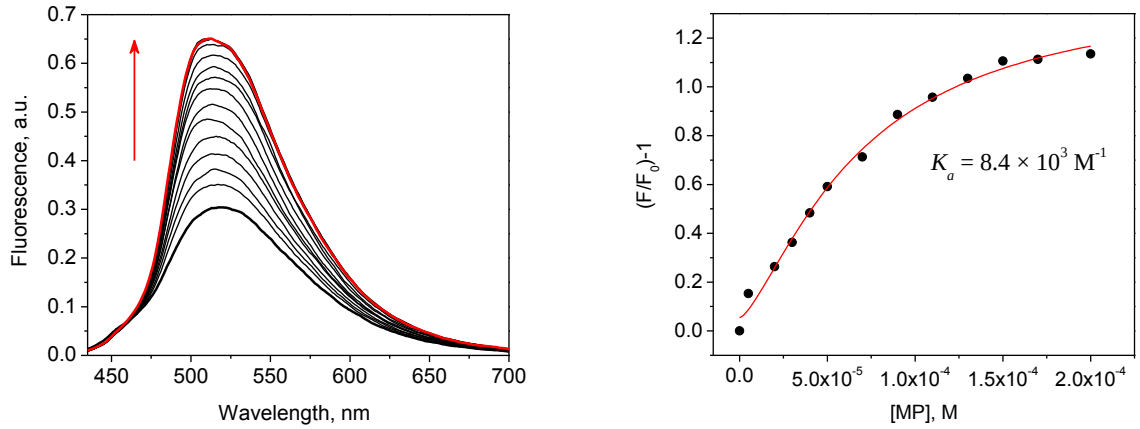

Fig. S24 Fluorescence spectra of **4** (10 μM) upon the addition of MP in DMSO. λ_{ex} = 400 nm. [MP] = 0 – 0.20 mM.

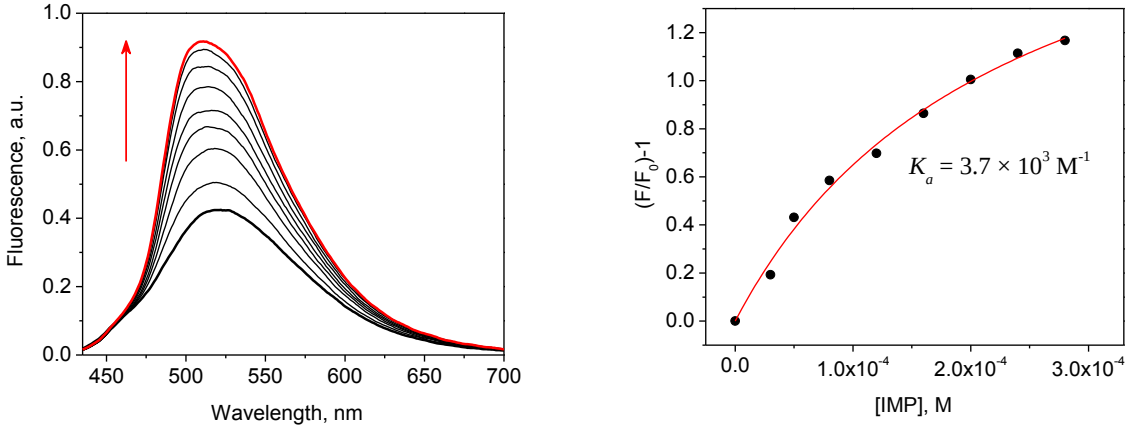

Fig. S25 Fluorescence spectra of **4** (10 μM) upon the addition of IMP in DMSO. λ_{ex} = 400 nm. [IMP] = 0 – 0.30 mM.

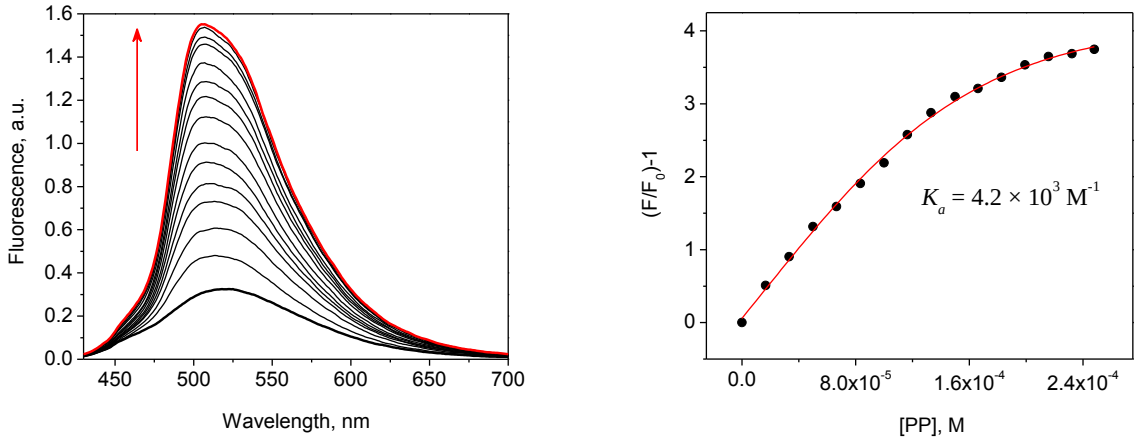

Fig. S26 Fluorescence spectra of **4** (10 μM) upon the addition of PP in DMSO. λ_{ex} = 400 nm. [PP] = 0 – 0.24 mM.

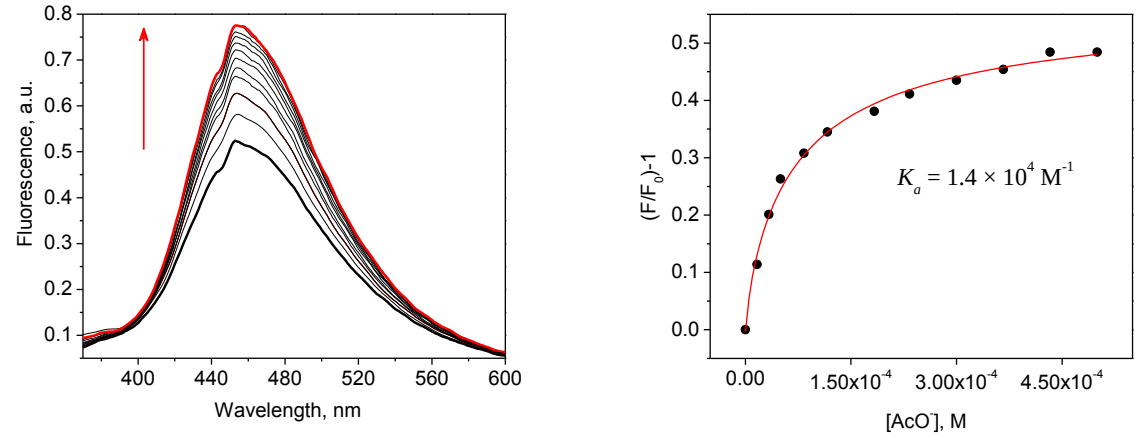

Fig. S27 Fluorescence spectra of **5** (10 μM) upon the addition of AcO^- in DMSO. λ_{ex} = 330 nm. [AcO^-] = 0 – 47 μM.

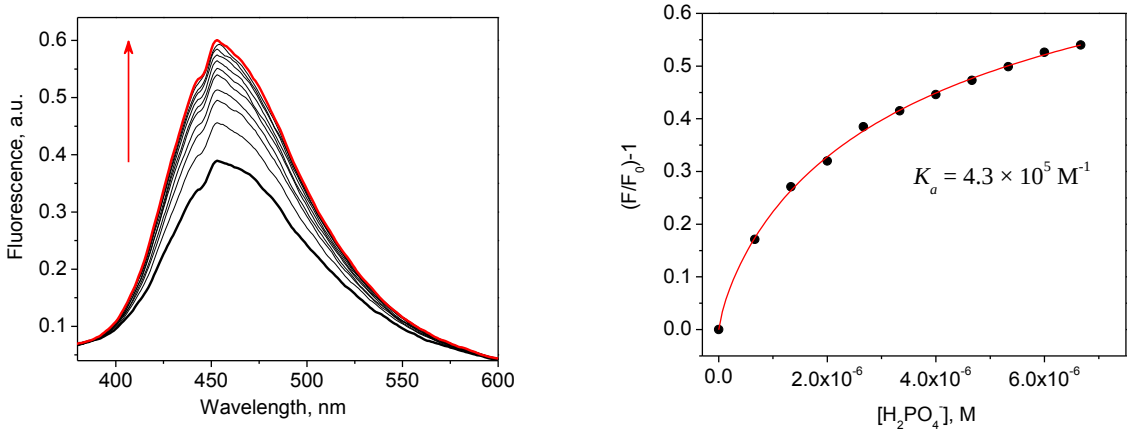

Fig. S28 Fluorescence spectra of **5** (10 μM) upon the addition of $H_2PO_4^-$ in DMSO. λ_{ex} = 330 nm. [$H_2PO_4^-$] = 0 – 7 μM.

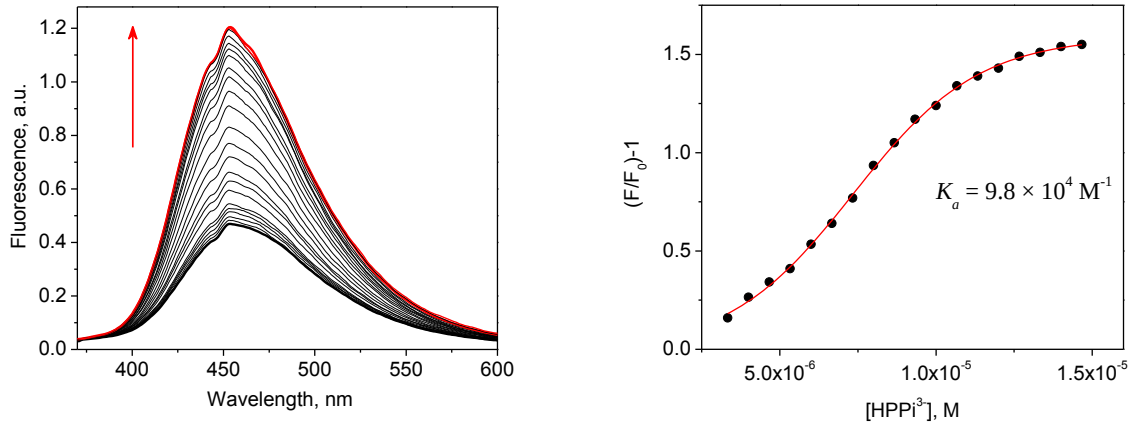

Fig. S29 Fluorescence spectra of **5** (10 μM) upon the addition of $HPPi^{3-}$ in DMSO. λ_{ex} = 330 nm. [$HPPi^{3-}$] = 0 – 15 μM.

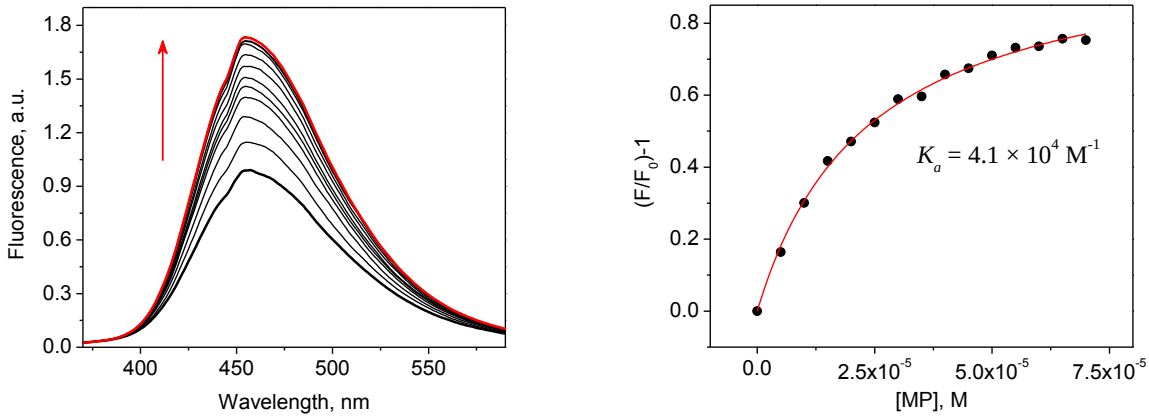

Fig. S30 Fluorescence spectra of **5** (10 μM) upon the addition of MP in DMSO. λ_{ex} = 330 nm. [MP] = 0 – 75 μM.

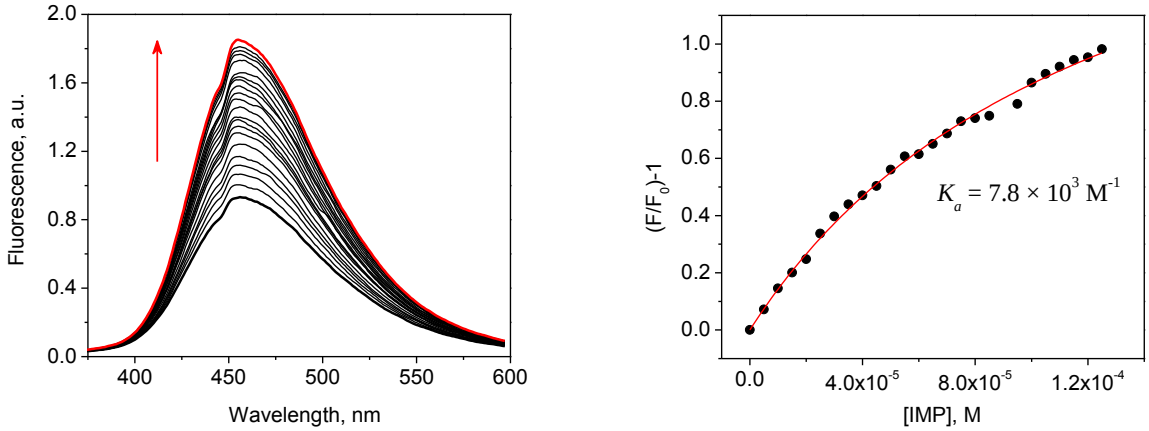

Fig. S31 Fluorescence spectra of **5** (10 μM) upon the addition of IMP in DMSO. λ_{ex} = 330 nm. [IMP] = 0 – 0.30 mM.

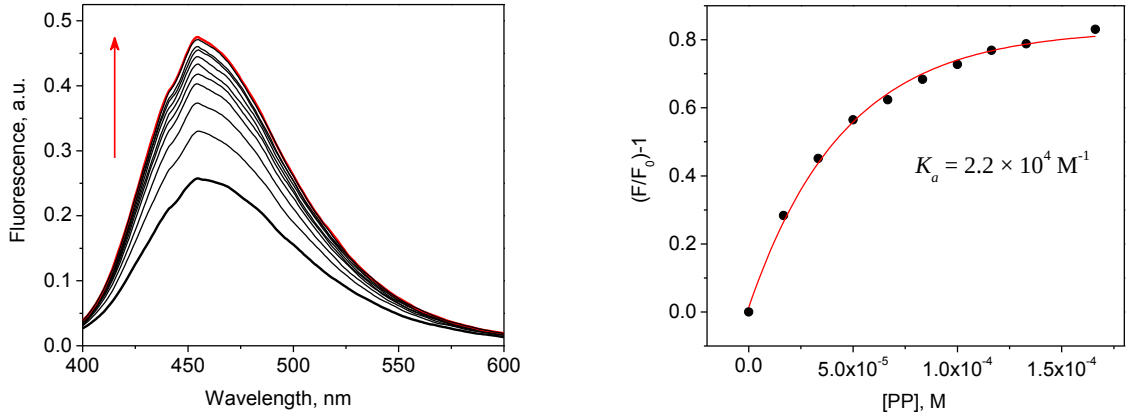

Fig. S32 Fluorescence spectra of **5** (10 μM) upon the addition of PP in DMSO. λ_{ex} = 330 nm. [IMP] = 0 – 0.16 mM.

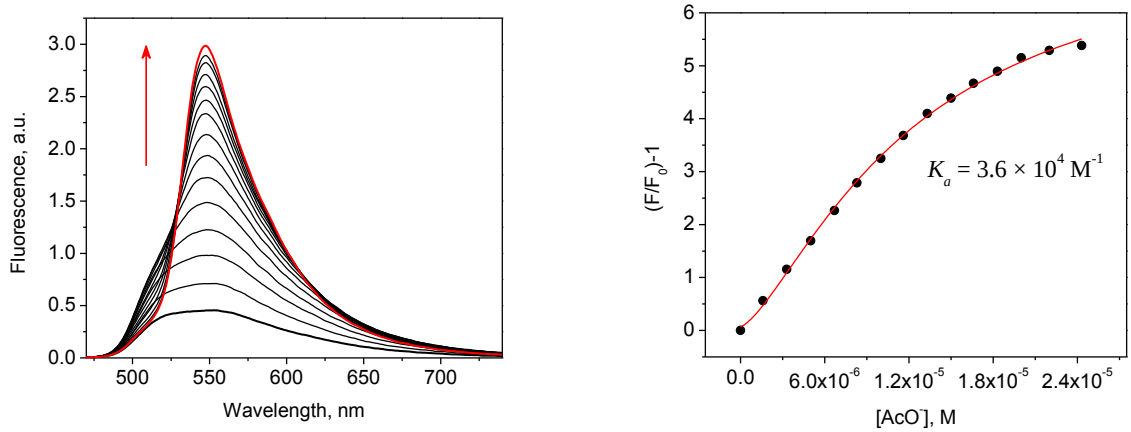

Fig. S33 Fluorescence spectra of **6** (10 μM) upon the addition of AcO^- in DMSO. λ_{ex} = 450 nm. [AcO^-] = 0 – 25 μM.

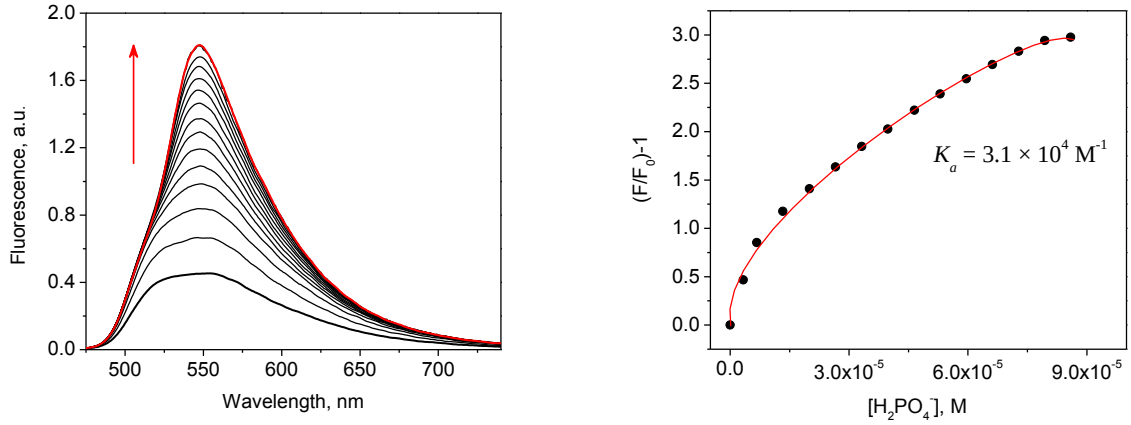

Fig. S34 Fluorescence spectra of **6** (10 μM) upon the addition of $H_2PO_4^-$ in DMSO. λ_{ex} = 450 nm. $[H_2PO_4^-]$ = 0 – 90 μM.

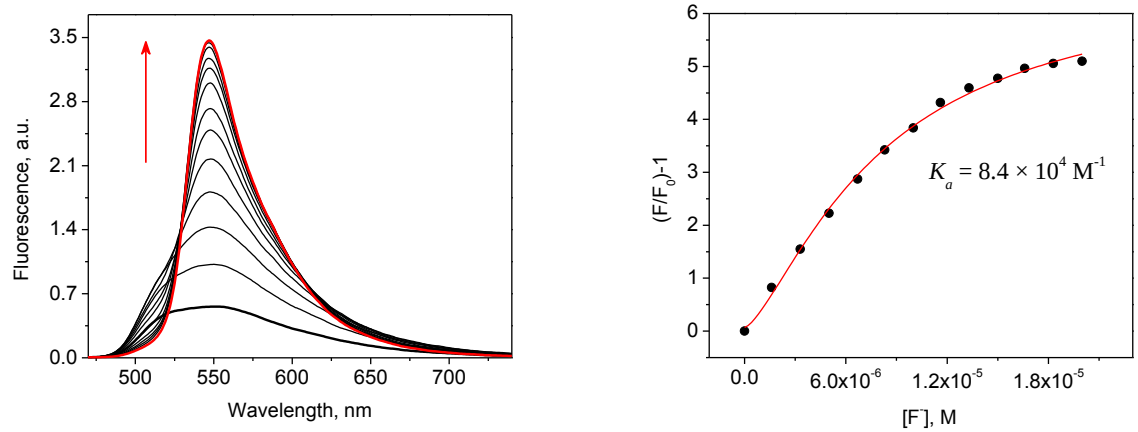

Fig. S35 Fluorescence spectra of **6** (10 μM) upon the addition of F^- in DMSO. λ_{ex} = 450 nm. $[H_2PO_4^-]$ = 0 – 20 μM.

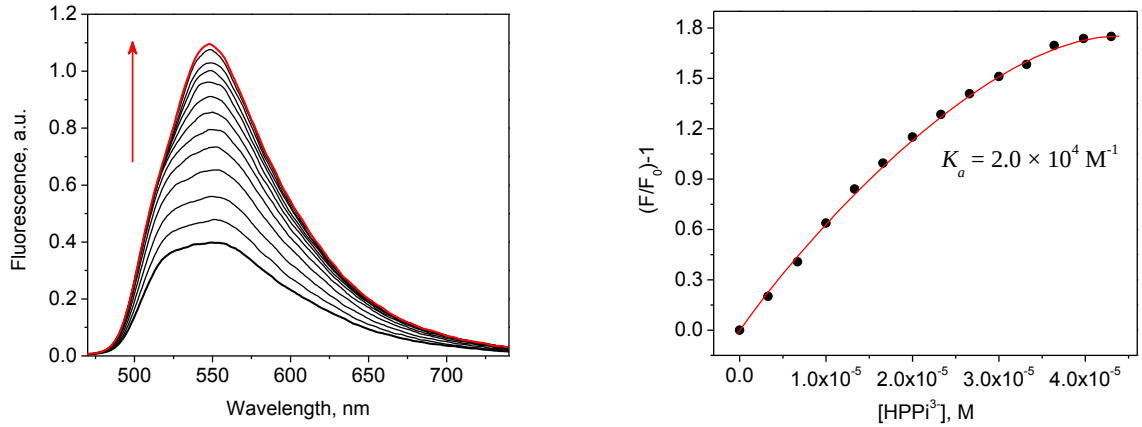

Fig. S36 Fluorescence spectra of **6** (10 μM) upon the addition of $HPPi^{3-}$ in DMSO. λ_{ex} = 450 nm. $[H_2PO_4^-]$ = 0 – 40 μM.

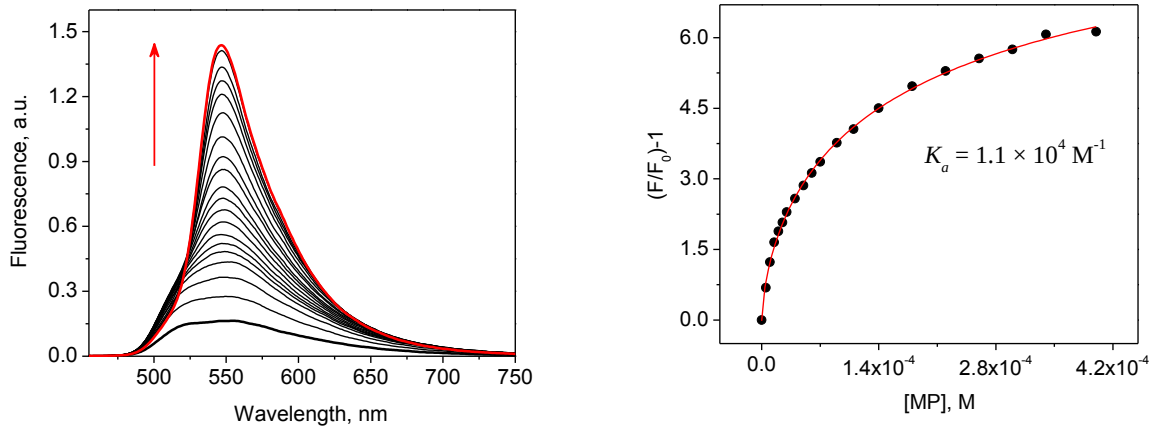

Fig. S37 Fluorescence spectra of **6** (10 μM) upon the addition of MP in DMSO. λ_{ex} = 450 nm. [MP] = 0 – 0.42 mM.

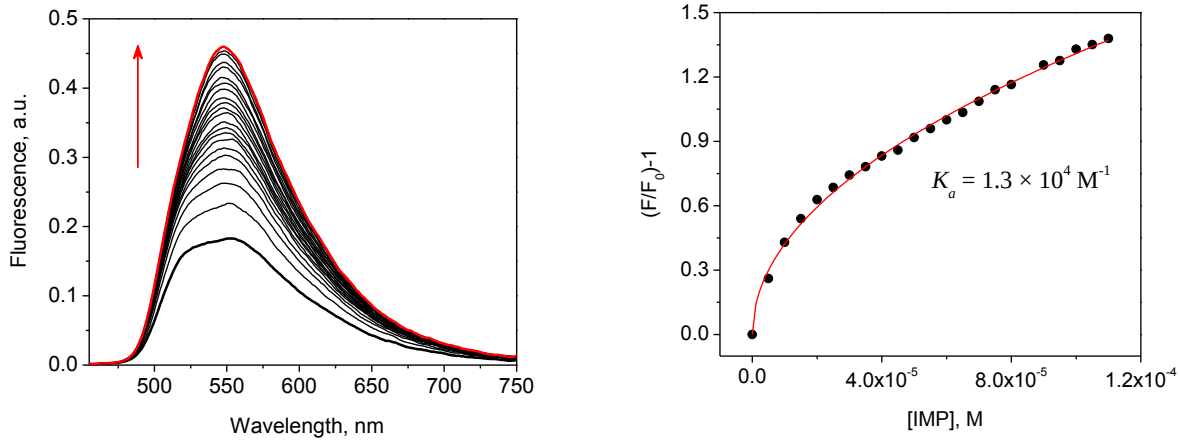

Fig. S38 Fluorescence spectra of **6** (10 μM) upon the addition of IMP in DMSO. λ_{ex} = 450 nm. [IMP] = 0 – 0.12 mM.

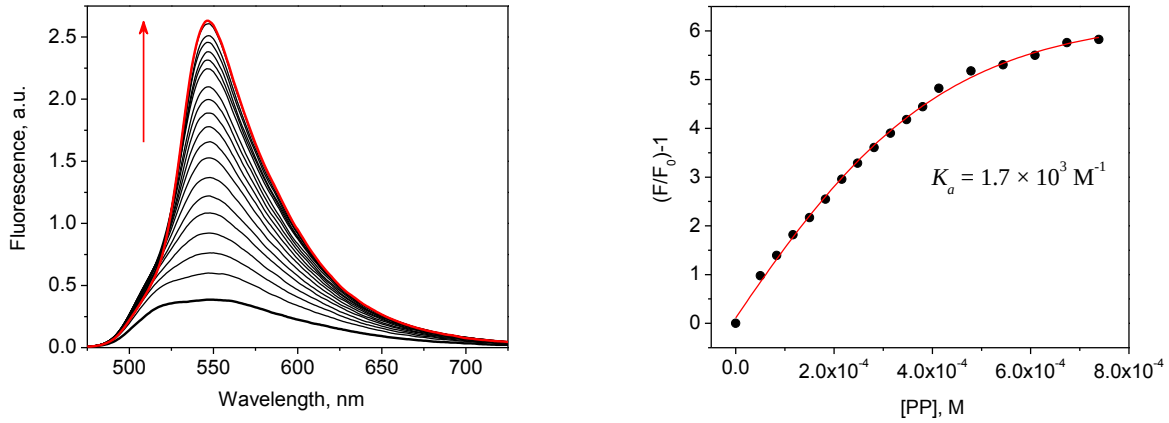

Fig. S39 Fluorescence spectra of **6** (10 μM) upon the addition of PP in DMSO. λ_{ex} = 450 nm. [PP] = 0 – 0.80 mM.

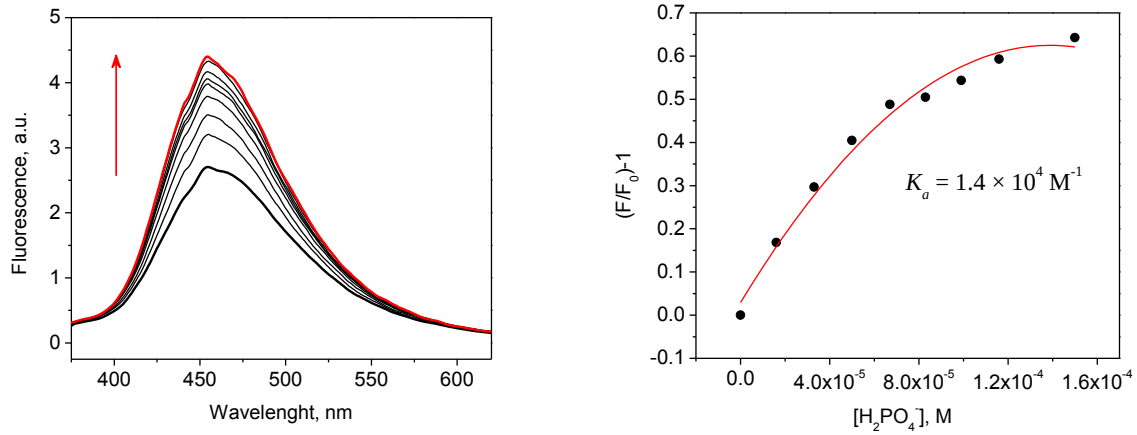

Fig. S40 Fluorescence spectra of **7** (10 μM) upon the addition of $H_2PO_4^-$ in DMSO. λ_{ex} = 330 nm. $[H_2PO_4^-]$ = 0 – 0.16 mM.

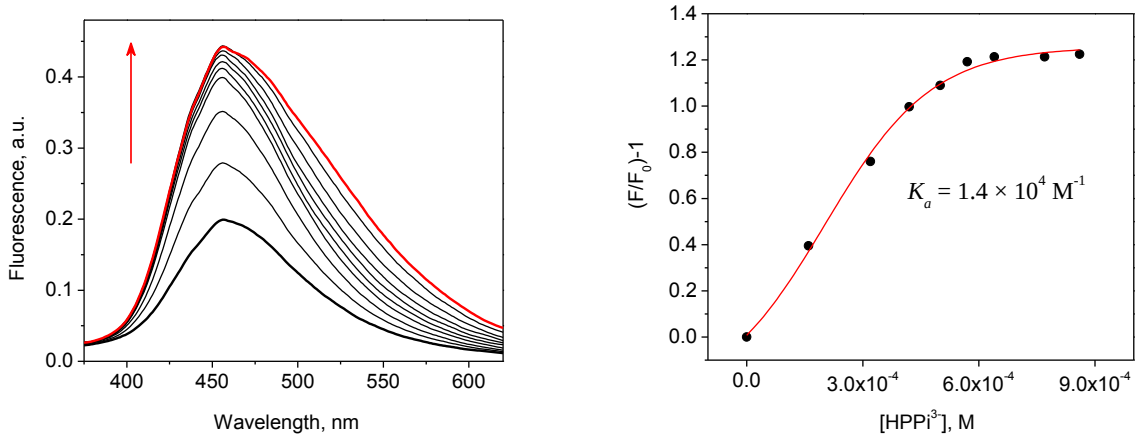

Fig. S41 Fluorescence spectra of **7** (10 μM) upon the addition of $HPPi^{3-}$ in DMSO. λ_{ex} = 330 nm. $[HPPi^{3-}]$ = 0 – 0.90 mM.

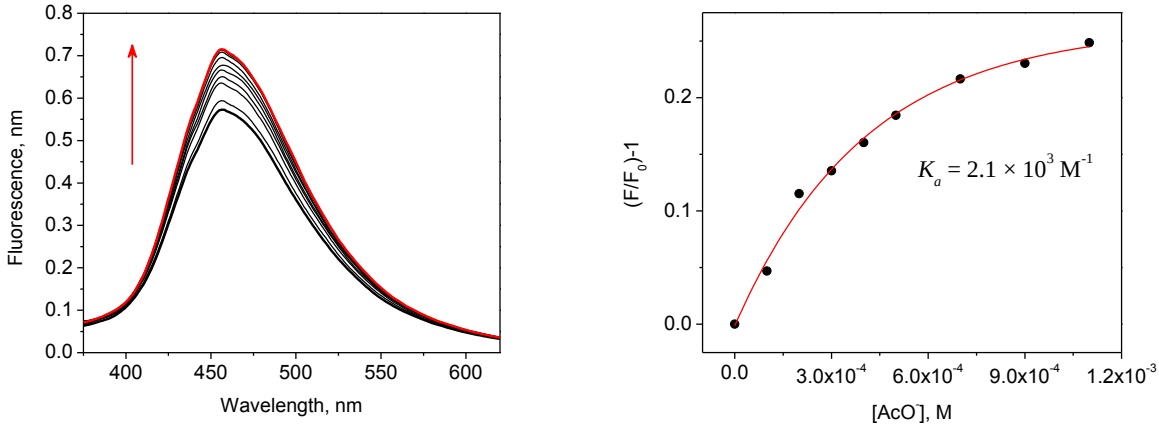

Fig. S42 Fluorescence spectra of **7** (10 μM) upon the addition of AcO^- in DMSO. λ_{ex} = 330 nm. $[AcO^-]$ = 0 – 1.2 mM.

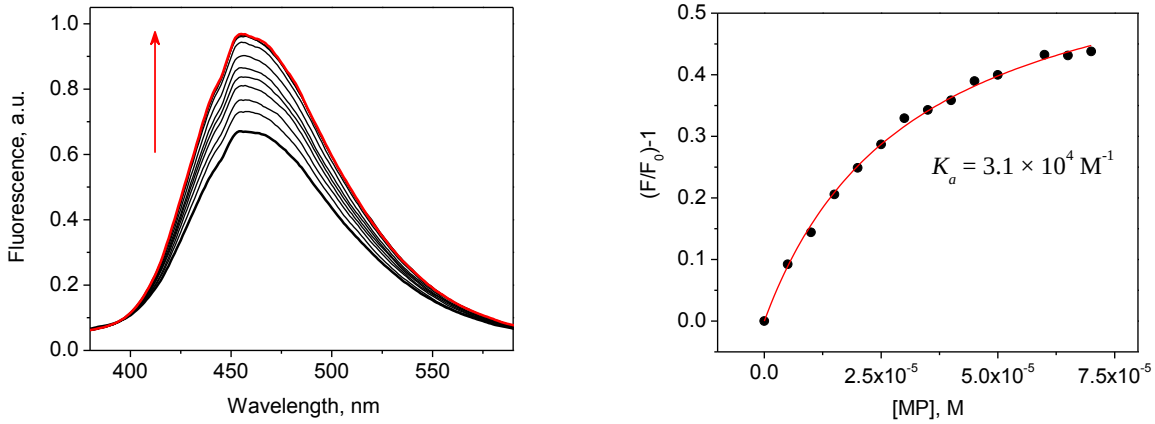

Fig. S43 Fluorescence spectra of **7** (10 μM) upon the addition of MP in DMSO. λ_{ex} = 330 nm. [MP] = 0 – 75 μM.

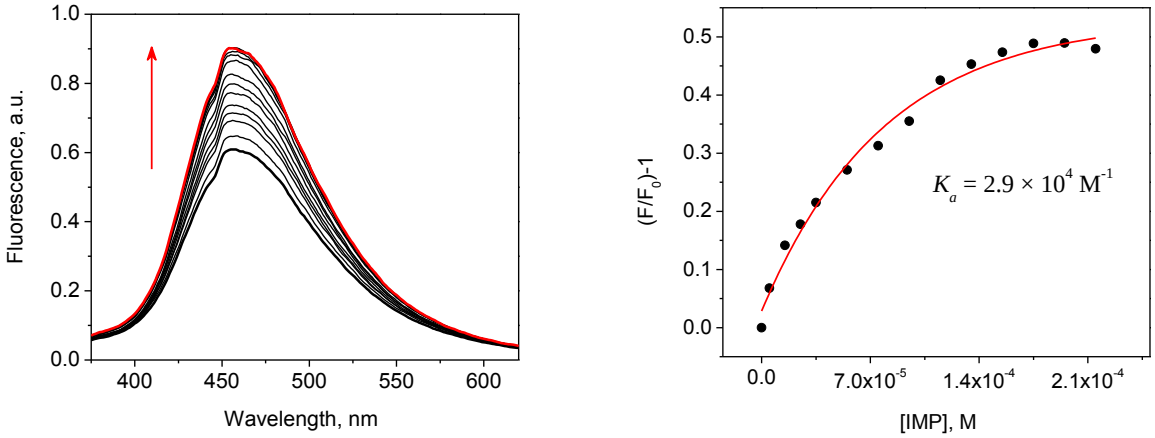

Fig. S44 Fluorescence spectra of **7** (10 μM) upon the addition of IMP in DMSO. λ_{ex} = 330 nm. [IMP] = 0 – 0.21 mM.

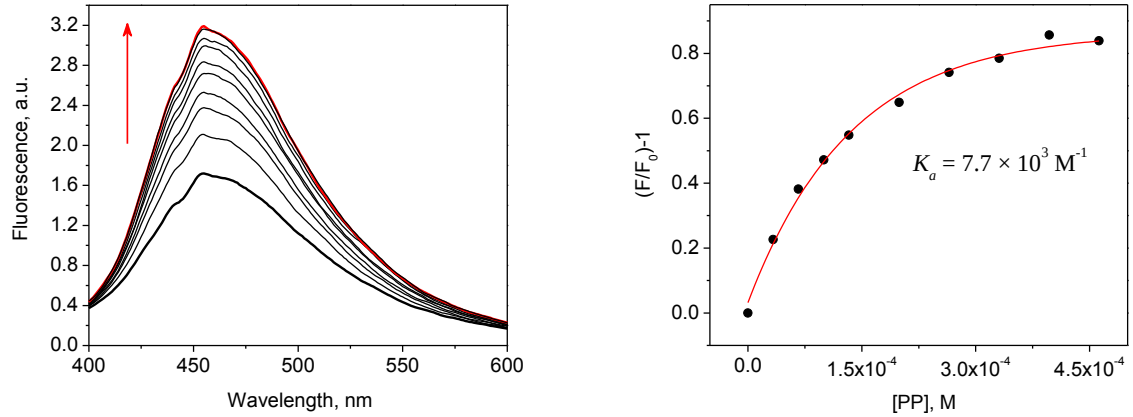

Fig. S45 Fluorescence spectra of **7** (10 μM) upon the addition of PP in DMSO. λ_{ex} = 330 nm. [PP] = 0 – 0.45 mM.

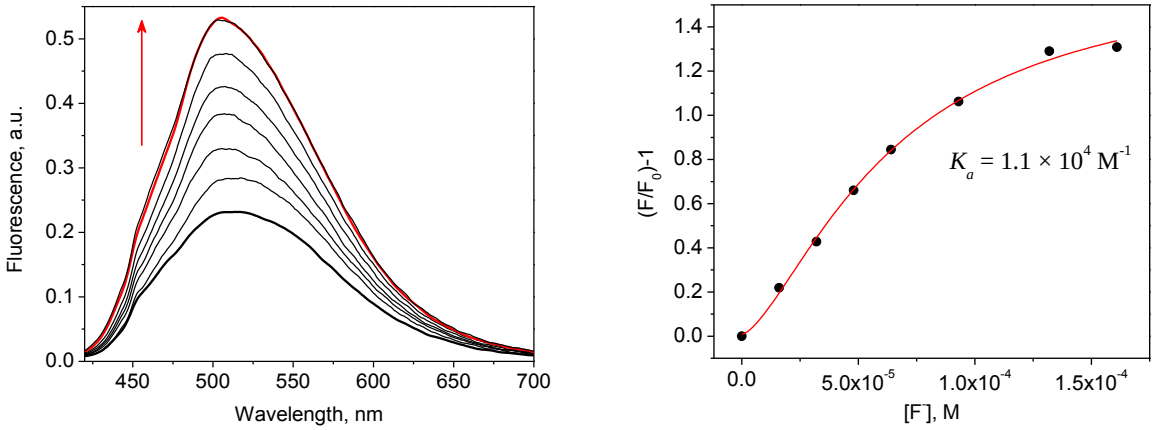

Fig. S46 Fluorescence spectra of **8** (10 μM) upon the addition of F^- in DMSO. λ_{ex} = 400 nm. [F^-] = 0 – 0.15 mM.

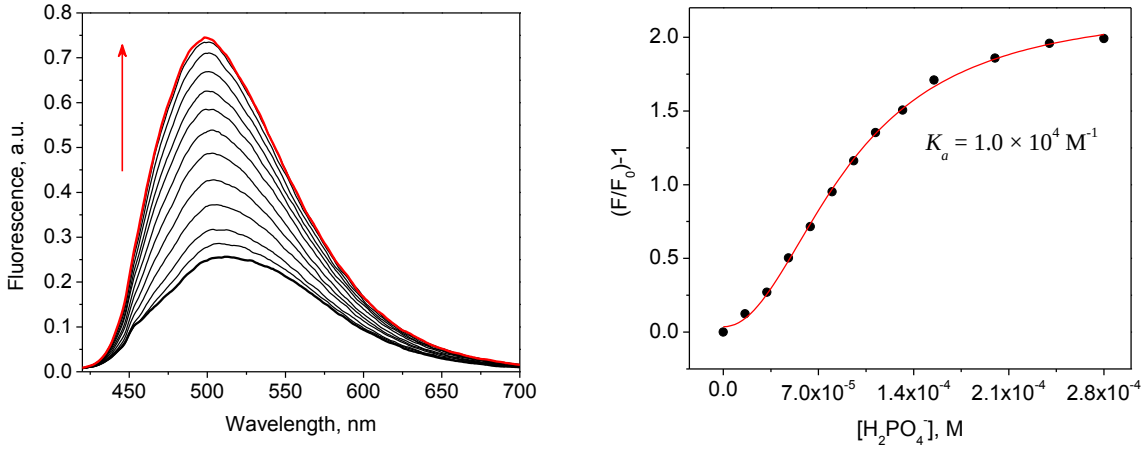

Fig. S47 Fluorescence spectra of **8** (10 μM) upon the addition of $H_2PO_4^-$ in DMSO. λ_{ex} = 400 nm. [$H_2PO_4^-$] = 0 – 0.30 mM.

Heatmap of Qualitative Microarray

Table S2 The heatmap of qualitative assay.

	S4	S5	S6	S7	S8	LUT
Ctrl	1	1	1	1	1	
Pi	0.998372	1.330445	4.498464	1.186065	1.003666	
PPi	0.182592	2.531575	8.297297	2.336053	0.467342	
AcO	0.966425	1.054009	8.258106	1.065771	0.996128	
Cl	0.981003	1.012382	0.943057	1.012299	0.98571	
F	0.807329	1.101052	8.896024	1.099552	0.984113	
MP	1.002719	1.286304	1.385011	1.132578	0.996419	
IMP	1.010773	1.524618	8.941814	1.337976	1.033733	

Linear Discriminant Analysis (LDA)

Table S3 The jackknifed classification matrix of qualitative assay (sensors **4**-**8**).

Jackknifed Classification Matrix

	AcO	Ctrl	F	IMP	MP	PPi	Pi	%correct
AcO	20	0	0	0	0	0	0	100
Ctrl	0	20	0	0	0	0	0	100
F	0	0	20	0	0	0	0	100
IMP	0	0	0	20	0	0	0	100
MP	0	0	0	0	20	0	0	100
PPi	0	0	0	0	0	20	0	100
Pi	0	0	0	0	0	0	20	100
Total	20	20	20	20	20	20	20	100

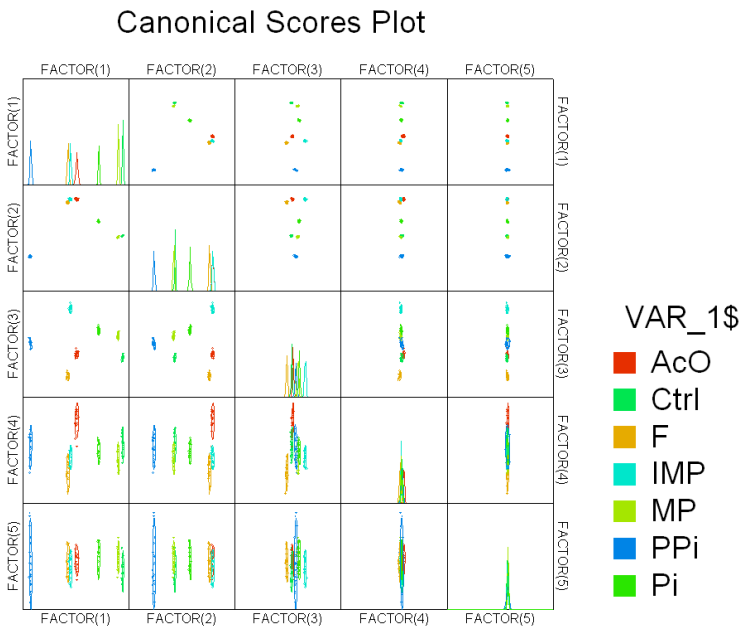

Fig. S48 The canonical scores plot of qualitative assay (sensors **4**-**8**).

Table S4 The jackknifed classification matrix of qualitative assay (sensors **4**, **5**, and **6**).

Jackknifed Classification Matrix								
	IMP	MP	AcO	Ctrl	F	PPi	Pi	%correct
IMP	20	0	0	0	0	0	0	100
MP	0	20	0	0	0	0	0	100
AcO	0	0	20	0	0	0	0	100
Ctrl	0	0	0	20	0	0	0	100
F	0	0	0	0	20	0	0	100
PPi	0	0	0	0	0	20	0	100
Pi	0	0	0	0	0	0	20	100
Total	20	20	20	20	20	20	20	100

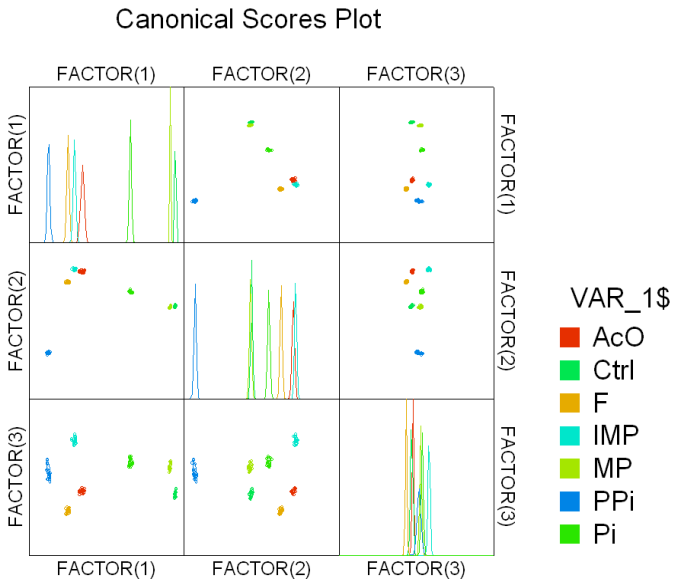

Fig. S49 The canonical scores plot of qualitative assay (sensors **4**, **5**, and **6**).

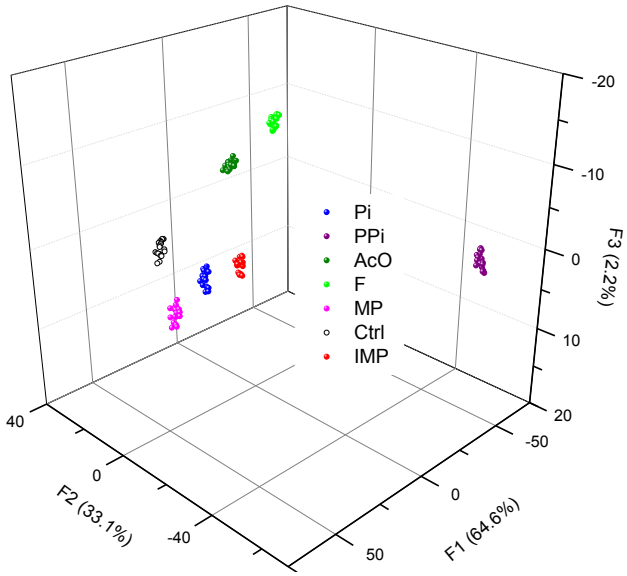

Fig. S50 The LDA of qualitative assay (sensors **4**, **5**, and **6**).

Table S5 The jackknifed classification matrix of qualitative assay (sensors **5** and **6**).

Jackknifed Classification Matrix

	AcO	Ctrl	F	IMP	MP	PPi	Pi	%correct
AcO	20	0	0	0	0	0	0	100
Ctrl	0	20	0	0	0	0	0	100
F	0	0	20	0	0	0	0	100
IMP	0	0	0	20	0	0	0	100
MP	0	0	0	0	20	0	0	100
PPi	0	0	0	0	0	20	0	100
Pi	0	0	0	0	0	0	20	100
Total	20	20	20	20	20	20	20	100

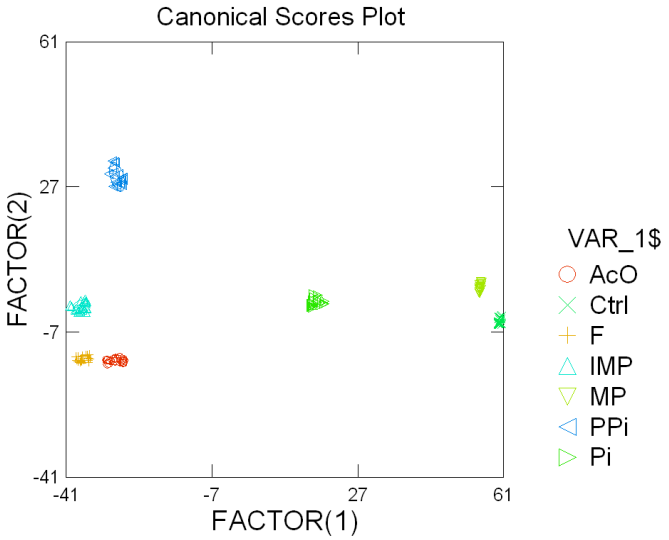

Fig. S51 The canonical scores plot of qualitative assay (sensors **5** and **6**).

Table S6 Input data set of the qualitative assay.

Analytes	Variables				
	4	**5**	**6**	**7**	**9**
Ctrl	41416.73	22846.52	12830.00	10741.73	65944.33
Ctrl	40794.00	23546.00	12306.17	11019.75	66525.26
Ctrl	41446.58	22934.00	12777.00	10925.79	64699.79
Ctrl	41178.95	22827.00	12448.00	10919.00	65857.55
Ctrl	41754.00	23303.41	12522.00	10329.43	65608.44
Ctrl	41404.00	23837.79	12818.00	10496.00	63776.85
Ctrl	41135.18	22782.11	12565.15	11302.00	64219.94
Ctrl	41526.00	23699.91	12815.29	10562.00	65166.00
Ctrl	41684.00	24074.00	12138.00	10435.48	64548.00
Ctrl	41336.15	22539.00	12069.76	11007.35	65260.00
Ctrl	40943.16	22556.68	12765.26	10666.00	64019.00
Ctrl	40671.00	22740.00	12514.00	10885.00	65985.00
Ctrl	42121.00	22941.11	12890.82	10947.89	64517.04
Ctrl	40828.00	23766.33	12465.09	11023.00	65486.00
Ctrl	40821.78	22637.19	12902.00	11056.00	64326.00
Ctrl	41878.00	23189.69	12471.95	10596.04	65745.00

Ctrl	41130.00	22700.00	12823.14	10618.84	64997.00
Ctrl	41551.00	23468.00	12406.23	11062.86	66421.00
Ctrl	41141.00	22552.00	12484.00	10993.48	66525.26
Ctrl	42068.39	23965.00	12279.00	10677.00	66102.00
Pi	42200.80	30638.95	57680.15	12841.36	65812.72
Pi	41307.93	30396.44	54512.00	12422.00	64857.00
Pi	41016.00	30689.00	55019.96	13154.51	65285.22
Pi	41194.05	32384.00	57168.47	12721.00	65281.00
Pi	41416.77	29881.00	57198.51	12907.00	64669.98
Pi	41047.00	30057.00	57147.00	13002.99	65613.76
Pi	40969.32	30159.01	57443.69	12852.47	65294.41
Pi	41296.00	31754.07	56979.49	12842.00	65663.76
Pi	41464.00	30634.00	57508.00	13253.00	65718.00
Pi	41156.00	31078.00	55991.97	12572.00	65355.00
Pi	40878.62	30015.94	57552.00	12843.00	65868.00
Pi	41475.22	32088.91	56046.00	12471.63	66259.61
Pi	41424.83	30455.29	57218.00	12897.93	66946.00
Pi	41371.00	30280.00	54631.00	12697.91	64879.00
Pi	41236.38	30748.53	54447.22	12514.00	66006.00
Pi	40578.31	30632.86	56087.91	12999.96	65397.46
Pi	41876.00	31247.75	57226.00	13212.00	66396.00
Pi	41269.00	30568.00	56955.00	13078.00	65020.00
Pi	40928.00	32066.00	56099.00	12567.60	65366.85
Pi	41378.00	30096.00	57511.53	12653.46	64827.00
PPi	7470.00	58758.03	104792.98	25042.00	30664.75
PPi	7779.25	60377.00	105473.00	24468.35	29038.00
PPi	7627.11	61455.00	105018.98	24320.28	31147.65
PPi	7338.00	58332.29	102935.69	25499.83	29797.00
PPi	7308.00	56985.00	103064.97	25838.28	30261.42
PPi	7553.59	56849.32	104450.00	24743.00	29407.00
PPi	8008.66	57634.00	104613.37	24346.47	29446.00
PPi	7398.62	59126.00	103839.00	24611.00	31377.00
PPi	7260.00	58221.11	102786.00	25838.00	30532.00
PPi	7587.32	58095.00	103126.16	25607.61	30121.08
PPi	7133.00	61278.83	104849.24	25435.36	31865.00
PPi	7356.00	59304.27	106222.96	25223.83	32080.01
PPi	7588.70	57200.17	103315.64	25303.40	30092.00
PPi	8094.04	57928.00	102875.00	25202.00	29915.96
PPi	7244.00	59520.49	105144.00	26158.00	29230.92
PPi	7570.42	61666.40	105491.00	24878.32	30736.95
PPi	7971.00	57105.00	104352.84	25771.00	30588.83
PPi	7400.68	57789.69	103400.00	25472.00	31403.00
PPi	7436.68	56857.00	105137.00	25932.97	31339.00
PPi	7847.14	57398.04	104147.00	25514.00	31178.08
AcO	39676.31	24706.16	106111.33	11252.17	65050.00
AcO	39525.00	24723.55	103495.00	11353.57	65063.00
AcO	40411.00	23964.68	105570.93	11294.76	65047.00
AcO	40246.22	24220.00	104015.68	11359.65	65222.00
AcO	39798.08	24616.16	102402.00	11676.00	65182.00
AcO	39475.00	24941.00	103978.27	11278.00	64268.96
AcO	39744.18	24017.86	102870.00	12016.71	65238.13
AcO	39614.00	23905.00	105886.90	11116.00	64724.00
AcO	39259.11	24664.00	105839.00	11553.32	66185.00

AcO	40096.00	23852.00	102087.37	11630.00	64250.63
AcO	39519.61	24691.84	105922.34	11819.00	65038.60
AcO	41080.00	24022.00	102048.00	11255.00	65788.00
AcO	40639.47	23862.40	102297.03	11336.00	64805.46
AcO	39747.18	24241.00	101949.00	11810.88	64393.00
AcO	40603.54	24722.52	104467.49	12009.00	64712.82
AcO	39375.00	24899.00	102956.00	11732.80	66856.82
AcO	40020.00	24156.95	102010.59	11476.00	64266.92
AcO	40189.33	24754.00	103917.00	11621.00	64142.00
AcO	39687.00	24478.00	102126.74	11236.96	65706.43
AcO	40362.00	24468.89	105236.00	11661.82	64733.18
F	33521.00	24765.04	110373.10	11887.82	64154.00
F	33628.00	26107.11	110257.48	11567.00	63486.32
F	33808.82	25102.00	112867.64	12403.99	63481.00
F	33454.00	25288.00	111535.00	12126.29	62887.00
F	32925.15	25073.00	112171.99	11542.71	66017.00
F	33036.00	26118.26	110729.00	11610.00	64348.00
F	32727.00	25205.00	112268.01	12257.00	64278.00
F	33342.27	26081.00	111868.26	11595.00	62957.88
F	33551.00	26142.00	111071.00	12118.24	63544.46
F	32727.46	25237.05	111645.84	12302.00	63896.00
F	33816.73	26059.51	112971.50	12316.00	64872.69
F	33742.60	24974.00	112514.00	11830.47	63813.78
F	33320.53	25363.66	110116.00	11593.02	64192.25
F	33247.38	26066.00	113445.71	11503.00	63986.00
F	32944.92	25544.00	112238.00	11620.18	65739.80
F	33925.46	25070.93	110398.00	11696.65	63907.63
F	33976.00	25336.00	112292.00	11785.00	66168.00
F	32622.00	25447.73	113301.00	11890.00	63932.00
F	33534.00	25544.96	110509.29	12110.00	64959.40
F	33673.00	25158.04	112916.63	12039.76	64364.00
MP	41547.98	29243.51	17418.00	12072.00	64149.72
MP	40962.00	28802.00	17509.99	12742.00	64375.00
MP	40977.71	30369.66	17575.00	12242.00	63906.00
MP	41629.00	30725.23	17060.77	12396.42	64909.00
MP	40897.81	29723.00	17318.00	12647.36	65012.00
MP	40872.00	30047.33	17417.00	12061.00	64725.00
MP	42301.02	29617.22	17654.00	12284.00	64671.66
MP	41507.03	29220.00	17443.55	12495.00	64470.00
MP	41639.86	29979.00	17521.89	12437.41	63989.36
MP	42331.98	30554.00	17233.00	12133.00	66793.00
MP	41220.40	29107.53	17573.46	12167.46	66497.00
MP	41186.00	29490.00	17659.00	12041.00	64357.07
MP	41200.00	29239.49	17324.55	12034.49	65153.77
MP	41329.00	29476.20	17139.00	12004.00	65388.00
MP	41090.00	29833.00	17272.98	12322.43	65478.57
MP	41604.91	30936.00	17291.00	11859.53	65629.74
MP	41900.00	30321.00	17218.44	12340.43	66793.13
MP	41415.00	30081.58	17150.02	12070.48	64992.00
MP	41359.22	29825.73	17677.59	12456.00	65006.00
MP	42106.00	28846.00	17583.38	12130.47	64757.46
IMP	42051.07	35741.00	111298.00	14426.15	66910.00
IMP	42144.00	34926.73	111934.00	14356.10	68286.00

IMP	41993.00	34944.00	111193.41	15004.56	66952.61
IMP	42122.38	36418.19	112523.76	14960.53	68592.00
IMP	41638.00	34389.04	113006.36	14368.00	67122.80
IMP	41548.84	35786.03	115066.05	14488.00	67111.00
IMP	42160.00	34980.00	113483.04	14217.01	68517.95
IMP	42250.95	34203.00	111231.00	14822.00	67447.00
IMP	41909.44	36114.00	111203.00	14204.00	67311.34
IMP	41226.42	34487.53	112594.00	14890.00	66698.00
IMP	41854.00	36003.11	111266.44	14246.00	68249.92
IMP	41133.00	34699.59	112429.02	14385.12	67942.00
IMP	41730.65	36213.16	111846.74	14335.09	66904.72
IMP	41480.00	35122.71	112678.00	14020.87	67714.90
IMP	41953.64	34855.00	111166.00	14467.18	66925.10
IMP	42036.00	34697.00	112176.37	14271.00	67406.00
IMP	41198.00	35260.00	112098.00	14530.00	67154.40
IMP	41565.92	35541.00	114698.92	14228.00	68190.00
IMP	42225.00	34863.41	113730.00	14503.21	67823.00
IMP	41516.00	36510.00	111374.01	14634.00	66516.44

Supporting information references

[1] K. J. Wallace, R. Hanes, E. Anslyn, J. Morey, K. V. Kilway, J. Siegel, *Synthesis*, 2005, 2080-2083.

[2] G.V. Zyryanov, M.A. Palacios, P. Anzenbacher *Angew. Chem. Int. Ed.*, 2007, **46**, 7849 –7852.

[3] DENZO-SMN. (1997). Z. Otwinowski and W. Minor, Methods in Enzymology, **276**: Macromolecular Crystallography, part A, 307 – 326, C. W. Carter, Jr. and R. M. Sweets, Editors, Academic Press.

[4] A. Altomare, M.C. Burla, M. Camalli, G. L. Cascarano, C. Giacovazzo, A. Guagliardi, A.G.G. Moliterni, G. Polidori, R. Spagna *J. Appl. Cryst.*, 1999, **32**, 115-119.

[5] G. M. Sheldrick, (1994). SHELXL97. Program for the Refinement of Crystal Structures. University of Gottingen, Germany.

[6] International Tables for X-ray Crystallography (1992). Vol. C, Tables 4.2.6.8 and 6.1.1.4, A. J. C. Wilson, Editor, Boston: Kluwer Academic Press.